in both primary hippocampal neurons and Ptk2 cells (*48*). The movement of mGluR5 was divided into two phases: (a) a diffusing phase in which mGluR5 moves quite freely, and (b) a confined phase in which mGluR5 is more trapped. While mGluR5 mobility increased with receptor activation, it decreased by coexpressing Homer-1b. In addition, the surface distribution of exogenous mGluR5 was uniform in both primary neurons and Ptk2 cells transfected with mGluR5 alone, whereas it was patchy in cells cotransfected with mGluR5 and Homer-1b. These results are compatible with the previously described effects of Homer proteins on the cell surface clustering of mGluR1a/5 (see above) and show that mGluR5 binding into larger protein complexes results in slower lateral receptor diffusion.

Animal Behavior

To establish the function of Homer proteins in *Drosophila* locomotor activity and behavioral plasticity, mutant flies were generated (*homer*^{R102}) in which the first two exons and half of the third exon of the *homer* gene were removed (*7*). A role for Homer in behavioral plasticity was verified by evaluating the performance of *homer*^{R102}-mutant males in a courtship-conditioning assay, an associative learning paradigm in *Drosophila* (*49*). Male flies react to olfactory, visual, and tactile signals with a complex and strong courtship toward females, and this behavior can be conditioned by previous experience. As compared with wild-type flies, *homer*^{R102} mutants were lacking behavioral plasticity and failed to form and/or retain the conditioning by the nonreceptive mated female (*7*). In addition, *homer*^{R102}-mutant flies exhibited higher levels of spontaneous locomotor activity. It thus appears that Homer, at least in *Drosophila*, is important in the development and function of neuronal networks underlying locomotion and behavioral plasticity.

Homer proteins have also been implicated in cocaine-induced behavioral plasticity in rats (*50*). Activation of mGluRs by dialyzing the group I mGluR agonist DHPG into the medial nucleus accumbens augments both the extracellular glutamate concentration and locomotor activity. In this system, repeated cocaine administration increased group I mGluR-induced glutamate release and locomotor activity in parallel with a reduction in Homer-1b/c protein.

Spine Maturation and Synaptic Function

Many of the regulatory proteins involved in the dynamic morphological rearrangement of spines are embedded within the PSD. Using quantitative morphometric analysis of spines in cultured hippocampal neurons, Shank overexpression was shown to promote the development and enlargement of spine heads (*3*). These changes did not occur when a Shank mutant was used that does not bind Homer-1b protein any more. Moreover, overexpression of this Shank mutant decreased the amount of endogenous Homer-1b in spines, and reduced the number of dendritic spines (*3*). While Homer-1b overexpression in the absence of Shank had no detectable effect on spine morphology, coexpression of both Shank and Homer-1b caused a more pronounced spine growth and increased the frequency of miniature excitatory postsynaptic currents (*3*). These data suggest that an unknown retrograde signal triggers the maturation of presynaptic function.

To study the synaptic function of Homer-1a and Homer-1c in hippocampal neurons, we used Semliki Forest virus vectors (*51,52*) to upregulate these proteins. We found that overexpression of Homer-1a enhanced AMPA receptor function and clustering, whereas it affected neither NMDA receptor function and clustering nor presynaptic glutamate release (*53*). In contrast to Homer-1a, Homer-1c overexpression did not alter synaptic transmission. While Homer-1a resulted in a greater AMPA-to-NMDA ratio in mEPSCs (recorded in the presence of tetrodotoxin), the NMDA component remained constant. In addition, the increase in AMPA-to-NMDA ratio caused by Homer-1a was higher for evoked EPSCs than for mEPSCs. We therefore proposed in

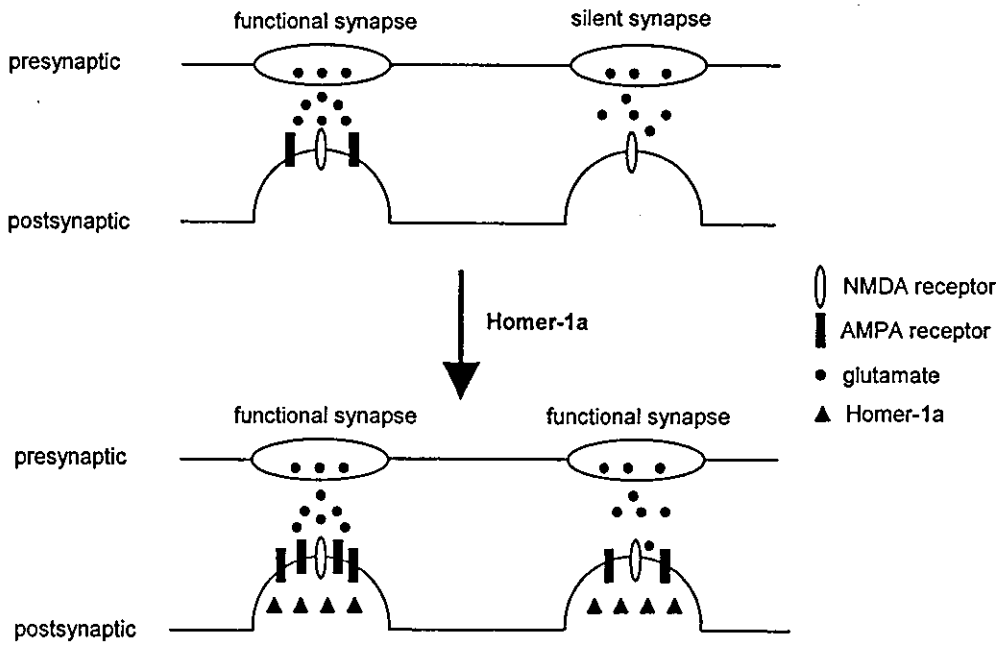

Fig. 3. Working model for the effect of Homer-1a on hippocampal synaptic transmission. Presynaptic release of glutamate into the synaptic cleft can activate two kinds of synapses: (a) functional synapses, i.e., synapses containing both NMDA and AMPA receptors (open and closed symbols, respectively), and (b) "silent synapses" that contain NMDA receptors but lack functional AMPA receptors. Overexpression of Homer-1a (triangles) induces an increase in the synaptic transmission without changing the glutamate release (circles). Our experiments lead to the conclusion that more AMPA receptors are expressed in functional synapses, but also in nonfunctional ones, which represents a conversion of silent synapses into functional ones.

our previous study *(53)* that Homer-1a promotes AMPA receptor insertion at both functional synapses (containing AMPA and NMDA receptors) and previously silent synapses (expressing only NMDA receptors; Fig. 3).

In contrast to our data, Sala et al. recently reported Homer-1a to inhibit rather than enhance hippocampal synaptic transmission *(54)*. In their study, Homer-1a overexpression caused shrinkage of dendritic spines and a decrease in both AMPA and NMDA receptor currents. The apparent contradiction between these and our data may result from different experimental protocols used. While we examined hippocampal slices prepared from postnatal day 6 (P6) rats and cultured for 2–3 wk (in the roller-tube configuration), Sala et al. employed slices from P8 rats at 4–6 d in culture (stationary on membranes). For dissociated hippocampal neurons, we used 3–4-wk-old cultures and Sala et al. 12-d-old cultures. Our experiments were thus conducted with more mature cultures, which might explain the discrepancy of the data. In addition, we employed conventional Semliki Forest virus vectors for gene transfer and analyzed the neurons at 1–2 d after transduction, whereas Sala et al. applied Ca^{2+} phosphate precipitation for dissociated neurons and a biolistic gene gun for slices and examined them at 4–5 and 2 d posttransfection, respectively (note that under physiological conditions Homer-1a protein is induced within few

hours of neuronal activation). Differences in transgene expression levels thus obtained with varying transfection techniques could also affect the experimental outcome. In any case, a positive feed-forward role, rather than a negative feedback function of Homer-1a in hippocampal synaptic transmission, seems to be a more straightforward explanation for Homer-1a being induced with protocols causing hippocampal long-term potentiation. In addition, our results agree with a recent report showing in the nucleus accumbens that downregulation of Homer-1b/c with antisense oligonucleotides specifically decreases the protein level of the AMPA receptor subunit GluR1 (*55*).

Conclusion

A rapidly increasing number of investigations provide data that support a role for Homer proteins in synaptic plasticity. The functions of Homer proteins result from their particular structural properties that permit them to interact with membrane receptors, such as mGluRs, but also with intracellular receptors, including Shank, IP_3Rs, and RyRs. It thus appears that Homer proteins not only are important in receptor scaffolding, but also modulate receptor activity. Intracellular Ca^{2+} is implicated in several mechanisms that lead to the potentiation of synapses, and Homer proteins have been shown to control intracellular Ca^{2+} homeostasis by regulating type I mGluRs, IP_3Rs, RyRs, TRPC channels, and voltage-gated Ca^{2+} channel activity. It is therefore probable that Homer proteins are also involved in hippocampal synaptic plasticity.

Acknowledgments

Our work was supported by grant no. 31–57125.99 from the Swiss National Science Foundation. We are grateful to Dr. Beat H. Gähwiler for helpful discussions and to Dr. Urs Gerber for comments on the manuscript.

References

1. Shiraishi Y., Mizutani A., Bito H., Fujisawa K., Narumiya S., Mikoshiba K., et al. (1999) Cupidin, an isoform of Homer/Vesl, interacts with the actin cytoskeleton and activated Rho family small GTPases and is expressed in developing mouse cerebellar granule cells. *J. Neurosci.* **19**, 8389–8400.
2. Kato A., Fukuda T., Fukazawa Y., Isojima Y., Fujitani K., et al. (2001) Phorbol esters promote postsynaptic accumulation of Vesl-1S/Homer-1a protein. *Eur. J. Neurosci.* **13**, 1292–1302.
3. Sala C., Piëch V., Wilson N.R., Passafaro M., Liu G., and Sheng M. (2001) Regulation of dendritic spine morphology and synaptic function by Shank and Homer. *Neuron* **31**, 115–130.
4. Usui S., Konno D., Hori K., Maruoka H., Okabe S., Fujikado T., et al. (2003) Synaptic targeting of PSD-Zip45 (Homer 1c) and its involvement in the synaptic accumulation of F-actin. *J. Biol. Chem.* **278**, 10,619–10,628.
5. Kato A., Ozawa F., Saitoh Y., Fukazawa Y., Sugiyama H., and Inokuchi K. (1998) Novel members of the Vesl/Homer family of PDZ proteins that bind metabotropic glutamate receptors. *J. Biol. Chem.* **273**, 23,969–23,975.
6. Xiao B., Tu J.C., Petralia R.S., Yuan J.P., Doan A., Breder C.D., et al. (1998) Homer regulates the association of group 1 metabotropic glutamate receptors with multivalent complexes of Homer-related, synaptic proteins. *Neuron* **21**, 707–716.
7. Diagana T.T., Thomas U., Prokopenko S.N., Xiao B., Worley P.F., and Thomas J.B. (2002) Mutation of *Drosophila homer* disrupts control of locomotor activity and behavioral plasticity. *J. Neurosci.* **22**, 428–436.
8. Brakeman P.R., Lanahan A.A., O'Brien R., Roche K., Barnes C.A., Huganir R.L., et al. (1997) Homer: a protein that selectively binds metabotropic glutamate receptors. *Nature* **386**, 284–288.
9. Kato A., Ozawa F., Saitoh Y., Hirai K., and Inokuchi K. (1997) *vesl*, a gene encoding VASP/Ena family related protein, is upregulated during seizure, long-term potentiation and synaptogenesis. *FEBS Lett.* **412**, 183–189.
10. Berke J.D., Paletzki R.F., Aronson G.J., Hyman S.E., and Gerfen C.R. (1998) A complex program of striatal gene expression induced by dopaminergic stimulation. *J. Neurosci.* **18**, 5301–5310.
11. Bottai D., Guzowski J.F., Schwarz M.K., Kang S.H., Xiao B., Lanahan A., et al. (2002) Synaptic

activity-induced conversion of intronic to exonic sequence in Homer 1 immediate early gene expression. *J. Neurosci.* **22,** 167–175.
12. Sun J., Tadokoro S., Imanaka T., Murakami S.D., Nakamura M., Kashiwada K., et al. (1998) Isolation of PSD-Zip45, a novel Homer/vesl family protein containing leucine zipper motifs, from rat brain. *FEBS Lett.* **437,** 304–308.
13. Soloviev M.M., Ciruela F., Chan W.-Y., and McIlhinney R.A.J. (2000) Mouse brain and muscle tissues constitutively express high levels of Homer proteins. *Eur. J. Biochem.* **267,** 634–639.
14. Kaja S., Yang S.-H., Wei J., Fujitani K., Liu R., Brun-Zinkernagel A.-M., et al. (2003) Estrogen protects the inner retina from apoptosis and ischemia-induced loss of Vesl-1L/Homer 1c immunoreactive synaptic connections. *Invest. Ophthalmol. Vis. Sci.* **44,** 3155–3162.
15. Sandonà D., Tibaldo E., and Volpe P. (2000) Evidence for the presence of two Homer 1 transcripts in skeletal and cardiac muscles. *Biochem. Biophys. Res. Commun.* **279,** 348–353.
16. Fanning A.S. and Anderson J.M. (1998) PDZ domains and the formation of protein networks at the plasma membrane. *Curr. Top. Microbiol. Immunol.* **228,** 209–233.
17. Hata Y., Nakanishi H., and Takai Y. (1998) Synaptic PDZ domain-containing proteins. *Neurosci. Res.* **32,** 1–7.
18. Gertler F.B., Niebuhr K., Reinhard M., Wehland J., and Soriano P. (1996) Mena, a relative of VASP and *Drosophila* Enabled, is implicated in the control of microfilament dynamics. *Cell* **87,** 227–239.
19. Haffner C., Jarchau T., Reinhard M., Hoppe J., Lohmann S.M., and Walter U. (1995) Molecular cloning, structural analysis and functional expression of the proline-rich focal adhesion and microfilament-associated protein VASP. *EMBO J.* **14,** 19–27.
20. Reinhard M., Halbrugge M., Scheer U., Wiegand C., Jockusch B.M., and Walter U. (1992) The 46/50 kDa phosphoprotein VASP purified from human platelets is a novel protein associated with actin filaments and focal contacts. *EMBO J.* **11,** 2063–2070.
21. Callebaut I., Cossart P., and Dehoux P. (1998) EVH1/WH1 domains of VASP and WASP proteins belong to a large family including Ran-binding domains of the RanBP1 family. *FEBS Lett.* **441,** 181–185.
22. Tu J.C., Xiao B., Yuan J.P., Lanahan A.A., Leoffert K., Li M., et al. (1998) Homer binds a novel proline-rich motif and links group 1 metabotropic glutamate receptors with IP3 receptors. *Neuron* **21,** 717–726.
23. Beneken J., Tu J.C., Xiao B., Nuriya M., Yuan J.P., Worley P.F., et al. (2000) Structure of the Homer EVH1 domain-peptide complex reveals a new twist in polyproline recognition. *Neuron* **26,** 143–154.
24. Tadokoro S., Tachibana T., Imanaka T., Nishida W., and Sobue K. (1999) Involvement of unique leucine-zipper motif of PSD-Zip45 (Homer 1c/vesl-1L) in group 1 metabotropic glutamate receptor clustering. *Proc. Natl. Acad. Sci. USA* **96,** 13,801–13,806.
25. Roche K.W., Tu J.C., Petralia R.S., Xiao B., Wenthold R.J., and Worley P.F. (1999) Homer 1b regulates the trafficking of group I metabotropic glutamate receptors. *J. Biol. Chem.* **274,** 25,953–25,957.
26. Coutinho V., Kavanagh I., Sugiyama H., Tones M.A., and Henley J.M. (2001) Characterization of a metabotropic glutamate receptor type 5-green fluorescent protein chimera (mGluR5-GFP): pharmacology, surface expression, and differential effects of Homer-1a and Homer-1c. *Mol. Cell Neurosci.* **18,** 296–306.
27. Ciruela F., Soloviev M.M., and McIlhinney R.A.J. (1999) Co-expression of metabotropic glutamate receptor type 1α with Homer-1a/Vesl-1S increases the cell surface expression of the receptor. *Biochem. J.* **341,** 795–803.
28. Ciruela F., Soloviev M.M., Chan W.-Y., and McIlhinney R.A.J. (2000) Homer-1c/Vesl-1L modulates the cell surface targeting of metabotropic glutamate receptor type 1α: evidence for an anchoring function. *Mol. Cell. Neurosci.* **15,** 36–50.
29. Ango F., Pin J.-P., Tu J.C., Xiao B., Worley P.F., Bockaert J., et al. (2000) Dendritic and axonal targeting of type 5 metabotropic glutamate receptor is regulated by Homer1 proteins and neuronal excitation. *J. Neurosci.* **20,** 8710–8716.
30. Berridge M.J. (1998) Neuronal calcium signaling. *Neuron* **21,** 13–26.
31. Satoh T., Ross C.A., Villa A., Supattapone S., Pozzan T., Snyder S.H., et al. (1990) The inositol 1,4,5,-trisphosphate receptor in cerebellar Purkinje cells: quantitative immunogold labeling reveals concentration in an ER subcompartment. *J. Cell Biol.* **111,** 615–624.
32. MacKrill J.J. (1999) Protein-protein interactions in intracellular Ca^{2+}-release channel function. *Biochem. J.* **337 (Pt 3),** 345–361.

33. Ango F., Robbe D., Tu J.C., Xiao B., Worley P.F., Pin J.P., et al. (2002) Homer-dependent cell surface expression of metabotropic glutamate receptor type 5 in neurons. *Mol. Cell. Neurosci.* **20,** 323–329.
34. Tu J.C., Xiao B., Naisbitt S., Yuan J.P., Petralia R.S., Brakeman P., et al. (1999) Coupling of mGluR/Homer and PSD-95 complexes by the Shank family of postsynaptic density proteins. *Neuron* **23,** 583–592.
35. Feng W., Tu J., Yang T., Vernon P.S., Allen P.D., Worley P.F., et al. (2002) Homer regulates gain of ryanodine receptor type 1 channel complex. *J. Biol. Chem.* **277,** 44,722–44,730.
36. Hwang S.-Y., Wei J., Westhoff J.H., Duncan R.S., Ozawa F., Volpe P., et al. (2003) Differential functional interaction of two Vesl/Homer protein isoforms with ryanodine receptor type 1: a novel mechanism for control of intracellular calcium signaling. *Cell Calcium* **34,** 177–184.
37. Westhoff J.H., Hwang S.-Y., Duncan R.S., Ozawa F., Volpe P., Inokuchi K., et al. (2003) Vesl/Homer proteins regulate ryanodine receptor type 2 function and intracellular calcium signaling. *Cell Calcium* **34,** 261–269.
38. Yuan J.P., Kiselyov K., Shin D.M., Chen J., Shcheynikov N., Kang S.H., et al. (2003) Homer binds TRPC family channels and is required for gating of TRPC1 by IP_3 receptors. *Cell* **114,** 777–789.
39. Montell C., Birnbaumer L., and Flockerzi V. (2003) The TRP channels, a remarkably functional family. *Cell* **108,** 595–598.
40. McNiven M.A., Cao H., Pitts K.R., and Yoon Y. (2000) The dynamin family. *Trends Biochem. Sci.* **25,** 115–120.
41. Gray N.W., Fourgeaud L., Huang B., Chen J., Cao H., Oswald B., et al. (2003) Dynamin 3 is a component of the postsynapse, where it interacts with mGluR5 and Homer. *Curr. Biol.* **13,** 510–515.
42. Minakami R., Kato A., and Sugiyama H. (2000) Interaction of Vesl-1L/Homer 1c with synatxin 13. *Biochem. Biophys. Res. Commun.* **272,** 466–471.
43. Kammermeier P.J., Xiao B., Tu J.C., Worley P.F., and Ikeda S.R. (2000) Homer proteins regulate coupling of group I metabotropic glutamate receptors to N-type calcium and M-type potassium channels. *J. Neurosci.* **20,** 7238–7245.
44. Herlitze S., Garcia D.E., Mackie K., Hille B., Scheuer T., and Catterall W.A. (1996) Modulation of Ca^{2+} channels by G-protein beta gamma subunits. *Nature* **380,** 258–262.
45. Charpak S., Gähwiler B.H., Do K.Q., and Knöpfel T. (1990) Potassium conductances in hippocampal neurons blocked by excitatory amino-acid neurotransmitters. *Nature* **347,** 765–767.
46. Ango F., Prézeau L., Muller T., Tu J.C., Xiao B., Worley P.F., et al. (2001) Agonist-independent activation of metabotropic glutamate receptors by the intracellular protein Homer. *Nature* **411,** 962–965.
47. Foa L., Rajan I., Haas K., Wu G.-Y., Brakeman P., Worley P., et al. (2001) The scaffold protein, Homer1b/c, regulates axon pathfinding in the central nervous system *in vivo*. *Nat. Neurosci.* **4,** 499–506.
48. Sergé A., Fourgeaud L., Hémar A., and Choquet D. (2003) Receptor activation and Homer differentially control the lateral mobility of metabotropic glutamate receptor 5 in the neuronal membrane. *J. Neurosci.* **22,** 3910–3920.
49. Kamyshev N.G., Iliadi K.G., and Bragina J.V. (1999) *Drosophila* conditioned courtship: two ways of testing memory. *Learn. Mem.* **6,** 1–20.
50. Swanson C.J., Baker D.A., Carson D., Worley P.F., and Kalivas P.W. (2001) Repeated cocaine administration attenuates group I metabotropic glutamate receptor-mediated glutamate release and behavioral activation: a potential role for Homer. *J. Neurosci.* **21,** 9043–9052.
51. Ehrengruber M.U. (2002) Alphaviral vectors for gene transfer into neurons. *Mol. Neurobiol.* **26,** 183–201.
52. Ehrengruber M.U. (2002) Alphaviral gene transfer in neurobiology. *Brain Res. Bull.* **59,** 13–22.
53. Hennou S., Kato A., Schneider E.M., Lundstrom K., Gähwiler B.H., Inokuchi K., et al. (2003) Homer-1a/Vesl-1S enhances hippocampal synaptic transmission. *Eur. J. Neurosci.* **18,** 811–819.
54. Sala C., Futai K., Yamamoto K., Worley P.F., Hayashi Y., and Sheng M. (2003) Inhibition of dendritic spine morphogenesis and synaptic transmission by activity-inducible protein Homer1a. *J. Neurosci.* **23,** 6327–6337.
55. Ghasemzadeh M.B., Permenter L.K., Lake R., Worley P.F., and Kalivas P.W. (2003) Homer1 proteins and AMPA receptors modulate cocaine-induced behavioural plasticity. *Eur. J. Neurosci.* **18,** 1645–1651.
56. Morioka R., Kato A., Fueta Y., and Sugiyama H. (2001) Expression of *vesl-1S/homer-1a*, a gene associated with long-term potentiation, in the brain of the epileptic EI mouse. *Neurosci. Lett.* **313,** 99–101.

57. Park H.T., Kang E.K., and Bae K.W. (1997) Light regulates Homer mRNA expression in the rat suprachiasmatic nucleus. *Mol. Brain Res.* **52,** 318–322.
58. Nielsen H.S., Georg B., Hannibal J., and Fahrenkrug J. (2002) *Homer-1* mRNA in the rat suprachiasmatic nucleus is regulated differentially by the retinohypothalamic tract transmitters pituitary adenylate cyclase activating polypeptide and glutamate at time points where light phase-shifts the endogenous rhythm. *Brain Res. Mol. Brain Res.* **105,** 79–85.
59. Vazdarjanova A., McNaughton B.L., Barnes C.A., Worley P.F., and Guzowski J.F. (2002) Experience-dependent coincident expression of the effector immediate-early genes arc and Homer 1a in hippocampal and neocortical neuronal networks. *J. Neurosci.* **22,** 10,067–10,071.
60. Polese D., de Serpis A.A., Ambesi-Impiombato A., Muscettola G., and de Bartolomeis A. (2002) Homer 1a gene expression modulation by antipsychotic drugs: involvement of the glutamate metabotropic system and effects of D-cycloserine. *Neuropsychopharmacology* **27,** 906–913.
61. de Bartolomeis A., Aloj L., Ambesi-Impiombato A., Bravi D., Caracò C., Muscettola G., et al. (2002) Acute administration of antipsychotics modulates Homer striatal gene expression differentially. *Brain Res. Mol. Brain Res.* **98,** 124–129.
62. Ageta H., Kato A., Hatakeyama S., Nakayama K., Isojima Y., and Sugiyama H. (2001) Regulation of the level of Vesl-1S/Homer-1a proteins by ubiquitin-proteasome proteolytic systems. *J. Biol. Chem.* **276,** 15,893–15,897.
63. Ageta H., Kato A., Fukazawa Y., Inokuchi K., and Sugiyama H. (2001) Effects of proteasome inhibitors on the synaptic localization of Vesl-1S/Homer-1a proteins. *Mol. Brain Res.* **97,** 187–189.
64. Sato M., Suzuki K., and Nakanishi S. (2001) NMDA receptor stimulation and brain-derived neurotrophic factor upregulate homer 1a mRNA via the mitogen-activated protein kinase cascade in cultured cerebellar granule cells. *J. Neurosci.* **21,** 3797–3805.
65. Thomas U. (2002) Modulation of synaptic signalling complexes by Homer proteins. *J. Neurochem.* **81,** 407–413.

ELSEVIER

Neuroscience Letters 354 (2004) 143–147

Neuroscience Letters

www.elsevier.com/locate/neulet

Activity-inducible protein Homer1a/Vesl-1S promotes redistribution of postsynaptic protein Homer1c/Vesl-1L in cultured rat hippocampal neurons

Yuriko Inoue[a], Naoki Honkura[a], Akihiko Kato[a], Suchie Ogawa[a], Hiroshi Udo[a], Kaoru Inokuchi[b], Hiroyuki Sugiyama[a,*]

[a]*Department of Biology, Faculty of Science, Graduate School of Science, Kyushu University, 6-10-1 Hakozaki, Higashi-ku, Fukuoka 812-8581, Japan*
[b]*Mitsubishi-Kagaku Institute of Life Sciences, 11 Minamiooya, Machida, Tokyo 194-8511, Japan*

Received 11 August 2003; received in revised form 26 September 2003; accepted 30 September 2003

Abstract

In cultured rat hippocampal neurons, overexpression of Homer1a/Vesl-1S, an inducible protein upregulated by seizure or long-term potentiation, caused a reduction of punctate distribution of a postsynaptic protein Homer1c/Vesl-1L, without significant decrease in its total amount. Clusters of F-actin were also decreased. Treatments of cells with BDNF or a proteasome inhibitor, which cause increase in the expression level of endogenous Homer1a, also resulted in the reduction of Homer1c puncta. These results indicate that the accumulation of Homer1a, either exogenously expressed or endogenously induced, caused redistribution and dispersion of postsynaptic clusters of Homer1c and F-actin, suggesting an important role of Homer1a in synaptic remodeling.

Keywords: Long-term potentiation; Brain derived neurotrophic factor; F-actin; Homer; Vesl

Homer proteins (also termed Vesl proteins) are encoded by three distinct genes (*homer1–3*), each of which produces various alternative splice variants [6,13]. The Homer family proteins are categorized into two classes. One is a major class that includes the long splice variants of these genes such as Homer1b, Homer1c (or Vesl-1L), Homer2a/b and Homre3a/b. The other class includes the short splice variants, Homer1a (or Vesl-1S), Homer2c/d and Homer3c/d. The short variants lack the C-terminal half. Thus, Homer1c but not Homer1a can dimerize through a coiled-coil domain in the C-terminal region [6,11,13]. Homer1c is expressed constitutively, interacts with postsynaptic proteins and accumulates in postsynaptic regions. In contrast, Homer1a is expressed at low level in the resting state, is the only family member known to date to be induced by the electrical activity [3,7], and is accumulated in postsynaptic regions by various stimulations such as phorbol esters, KCl or BDNF treatments [4,5,10]. In the present study, we tried to find the physiological significance of Homer1a proteins. For this purpose, we either exogenously overexpressed Homer1a or induced the endogenous Homer1a. We found that the expression of Homer1a resulted in a significant alteration in the subcellular localization of Homer1c, in which postsynaptically accumulated Homer1c became dispersed by the Homer1a expression.

Experiments were performed on cultured rat hippocampal neurons [5]. Neurons were plated at a density of 2–3 × 10^4 cells/cm^2 onto coverslips coated with poly-L-lysine (1 mg/ml), and maintained in Neurobasal-A medium supplemented with 2% B-27 (Invitrogen) and 0.5 mM glutamine in a humidified atmosphere at 37 °C under 5% CO_2 for 14–17 days. The cDNAs encoding Homer1a or Homer1c were cloned in frame at *Eco*RI and *Bam*HI sites of pEYFP-C1 or pECFP-C1 (Clontech), or at *Eco*RI and *Sal*I sites of pEGFP-C2 (Clontech). Neurons were microinjected with the purified plasmid DNAs (2.5 mg/ml), and were examined 24–36 h later. Immunocytochemical analyses were performed as described [5]. Endogenous Homer1c was detected with anti-Homer1c rabbit antibody [5] and Cy5-conjugated anti-rabbit IgG goat antibody (1:100 dilution, Jackson Immuo Research).

* Corresponding author. Tel.: +81-92-642-2630; fax: +81-92-642-2645.
E-mail address: hsugiscb@mbox.nc.kyushu-u.ac.jp (H. Sugiyama).

0304-3940/03/$ - see front matter © 2003 Elsevier Ireland Ltd. All rights reserved.
doi:10.1016/j.neulet.2003.09.082

Specimens were examined using LSM510 laser scanning microscope (Zeiss). The laser intensity and the gain were adjusted to avoid saturation of the maximum pixel intensity (255) and photobleaching. Once optimized, individual samples were imaged at the same optical setting. Morphometric measurements were carried out with Image Browser (Zeiss). Neurons of pyramidal shape were morphologically identified, and 75 μm segments of one to three major dendrites, from 5 to 80 μm distal from the soma, were examined from each neuron. The Homer1c immunoreactive puncta on dendritic spines and shafts were defined as spots over 50% maximum pixel intensity at regions examined. The average fluorescent intensities were calculated for quantification.

Homer1c is a postsynaptic protein, and its molecular determinants are elucidated that cause its accumulation at postsynaptic regions [12]. The punctate postsynaptic distribution is observed not only for endogenous Homer1c, but also for exogenously expressed CFP-Homer1c fusion proteins (Figs. 1A–C). In contrast, YFP-Homer1a, which lacks one of these determinants, is distributed diffusely. Moreover, we found that endogenous Homer1c or CFP-

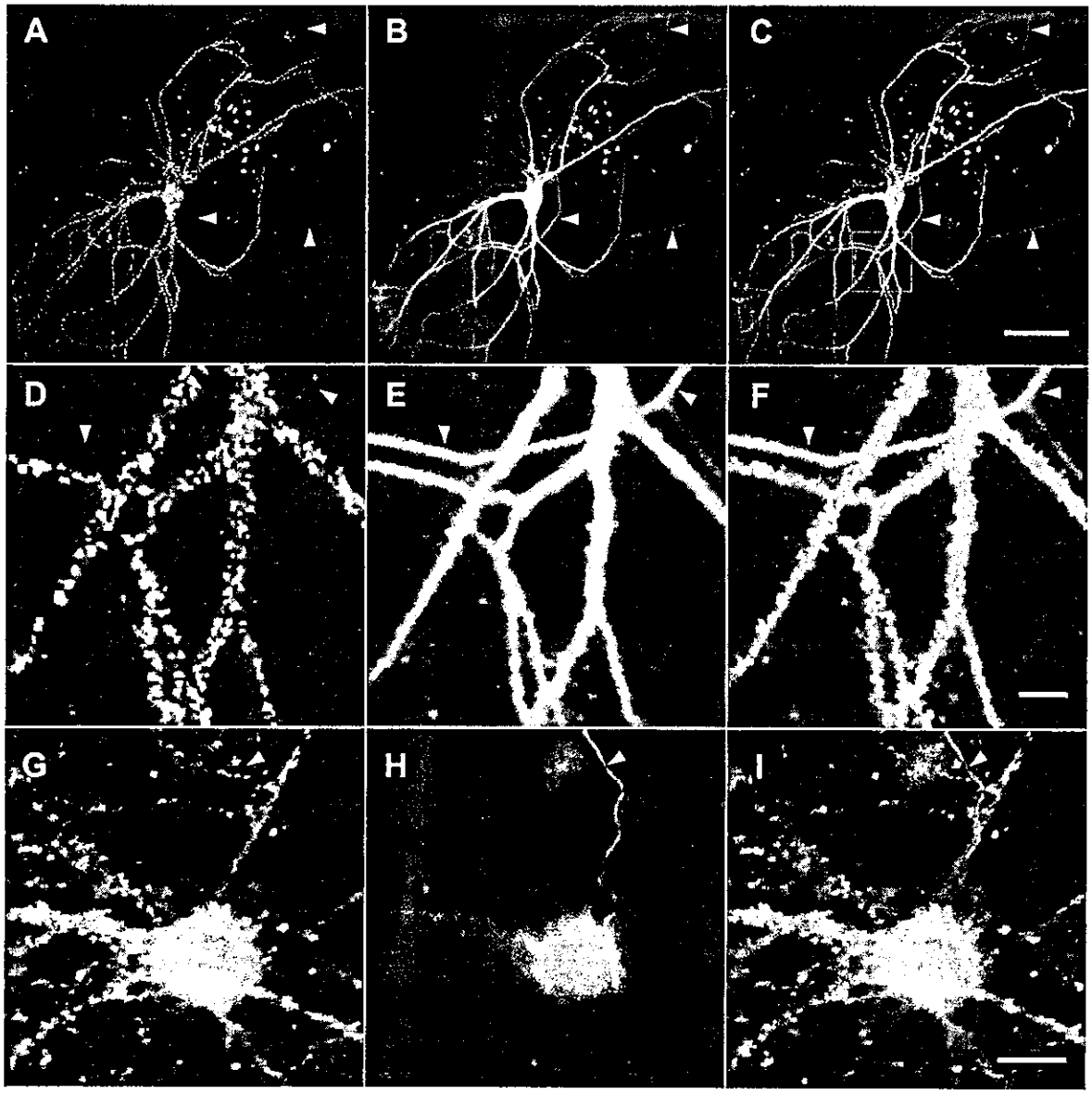

Fig. 1. Homer1c is excluded from axons and shows a punctate localization along dendrites. Hippocampal neurons were injected with plasmid DNAs encoding CFP-Homer1c (A and D, shown in green) and YFP-Homer1a (B and E, shown in red). Merged images show the distinct subcellular localization of Homer1a and 1c (C and F). Images of D–F represent the enlarged views of the outlined area in C. Neurons were stained with the anti-Homer1c antibody and with the anti-Tau-1 antibody (G and H, respectively; I shows the overlay). Arrowheads indicate the location of axons. Scale bars in Figures C, F and I represent 100, 10 and 20 μm, respectively.

Homer1c is excluded from axon, whereas Homer1a is distributed throughout neuronal processes including axon (Fig. 1). The neurites which excluded Homer1c are stained with an anti-Tau-1 antibody (Chemicon), indicating axons (Figs. 1G–I). We have also confirmed that these neurites are devoid of immunoreactivity against an anti-MAP2 antibody (data not shown). These results suggest that the C-terminal domain of Homer1c functions as the structural determinant for the local aggregation of Homer1c and also the exclusion of Homer1c from axons.

Next we examined the effects of overexpression of Homer1a on the distribution of Homer1c. Cultured neurons were injected with GFP or GFP-Homer1a DNA, and then the endogenous Homer1c was stained with anti-Homer1c antibodies. The numbers of Homer1c puncta along the dendrites were counted. As shown in Fig. 2, the number of Homer1c puncta was significantly reduced in neurons expressing GFP-Homer1a, compared to that in neurons expressing GFP.

These results may be explained by at least two mechanisms, either by the re-dispersion of aggregated Homer1c or by the suppression of the expression level of Homer1c. To distinguish these possibilities, we measured and compared the total amounts of Homer1c immunofluorescence in cells expressing GFP or GFP-Homer1a. The total fluorescence intensities in the dendrites examined for Homer1c puncta were measured, corrected for the background fluorescence, and normalized by the areas of the dendrites. The total amounts of Homer1c proteins were essentially unaffected by the expression of Homer1a (Fig. 2B), indicating that the overexpression of Homer1a caused the re-distribution of Homer1c proteins from aggregated states to diffusely dispersed states.

The EVH1 domain of Homer1a and Homer1c is known to be critical for their binding to group 1 metabotropic glutamate receptors or Shank family proteins. To elucidate the role of the EVH1 domain of Homer1a for the redistribution of Homer1c, we introduced an amino acid substitution within the EVH1 domain of Homer1a (W24A) [2,3] and overexpressed the GFP fusion of the mutant in neurons. As shown in Fig. 2, the expression of GFP-Homer1aW24A caused essentially no effects on the distribution of endogenous Homer1c clusters, indicating the critical importance of the EVH1 domain.

It has been reported that the interaction of Homer and Shank plays an important role in the morphogenesis of dendritic spines [9]. We therefore examined the effects of Homer1a overexpression on F-actin distribution which represents the morphology of spines. F-actin was detected with tetramethyl rhodamine isothiocyanate (TRITC)-phalloidin (1:1000 dilution, Molecular Probes). We found that the number of F-actin puncta also decreased by the overexpression of Homer1a (Fig. 3). This result is in accordance with the recent report by Sala et al. [8].

Our data indicate that the exogenous expression of Homer1a leads to the redistribution of Homer1c. Thus we expected that the induction of endogenous Homer1a would result in the dispersion of Homer1c clusters. We have

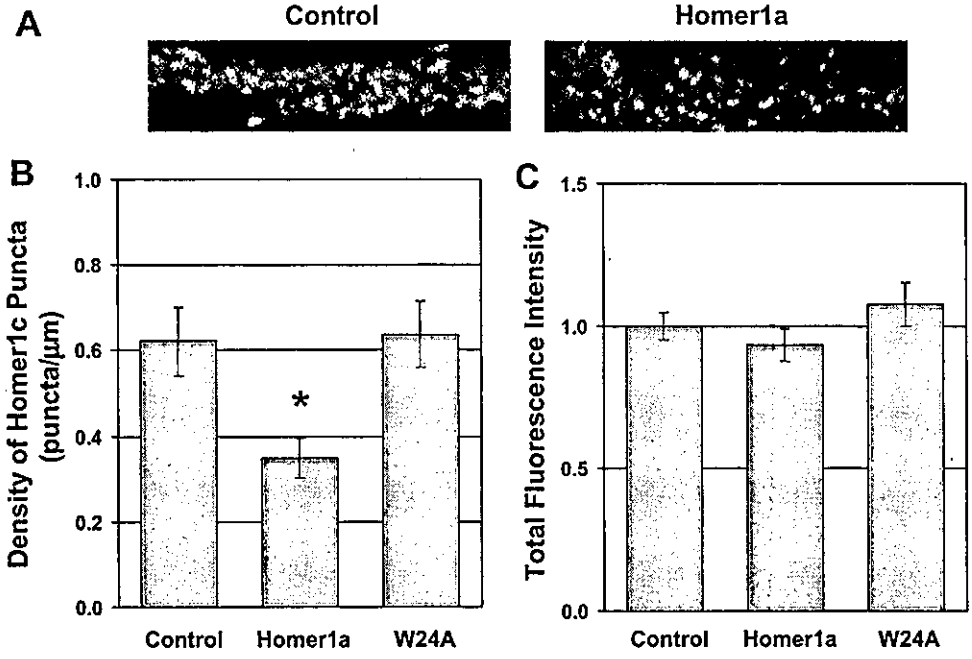

Fig. 2. Expression of Homer1a leads to dispersion of Homer1c clusters. Hippocampal neurons expressing GFP (control), GFP-Homer1a and GFP-Homer1aW24A were stained with the anti-Homer1c antibody. A. Localization of endogenous Homer1c in cells expressing GFP or GFP-Homer1a. B. Densities of Homer1c puncta along dendrites. C. Total fluorescence intensities of immuno-labeled Homer1c in dendrites, expressed relative to the control. Error bars represent ± SEM ($n = 43–72$ dendrites). *$P < 0.05$ by Student's t-test.

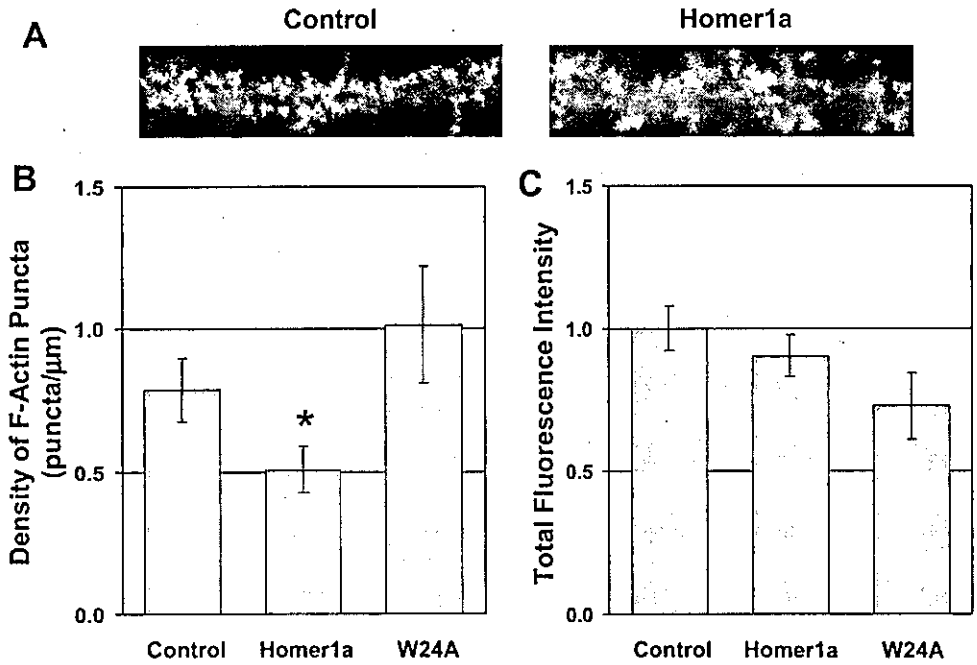

Fig. 3. Expression of Homer1a leads to redistribution of F-actin. Hippocampal neurons expressing GFP (control), GFP-Homer1a and GFP-Homer1aW24A were stained with TRITC-phalloidin. A. Localization of F-actin on cells expressing GFP or GFP-Homer1a. B. Densities of F-actin puncta along dendrites. C. Total fluorescence intensities of labeled F-actin in dendrites, expressed relative to the control. Error bars represent ± SEM ($n = 7–21$ dendrites). *$P < 0.05$ by Student's t-test.

previously shown that the level of Homer1a is usually kept low by rapid degradation through proteasome proteolytic systems, and that the inhibition of the proteasomes resulted in the accumulation of Homer1a [1]. We have also shown that the expression level of Homer1a is enhanced by phorbol esters or BDNF treatments [4,5]. Thus the treatments with BDNF or proteasome inhibitors such as MG132 cause enhanced expression of endogenous Homer1a. We therefore

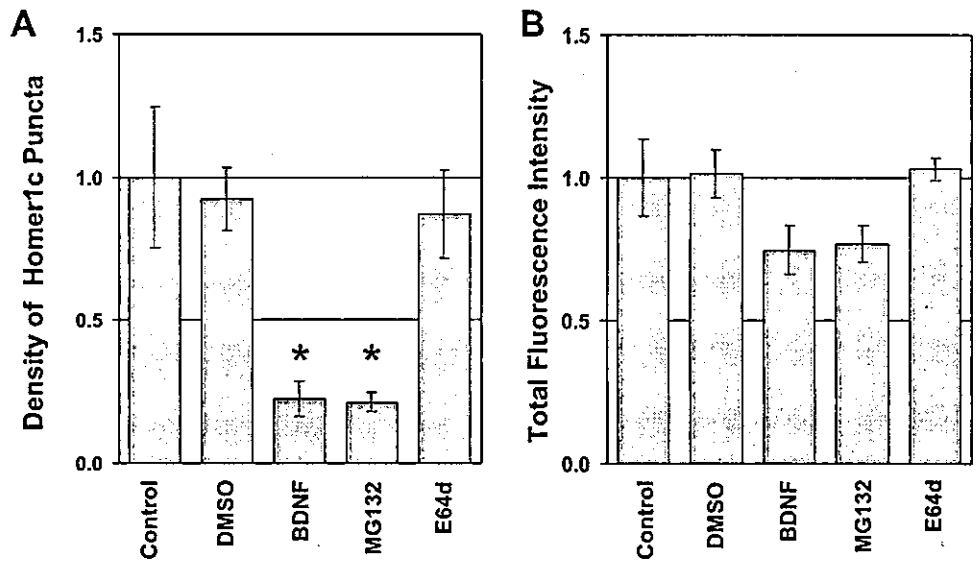

Fig. 4. Application of BDNF or MG132 induces redistribution of Homer1c clusters. Hippocampal neurons were treated with BDNF or a proteosome inhibitor MG132, which increases the amount of endogenous Homer1a, and the numbers of Homer1c puncta along dendrites were counted. E64d is an inhibitor of proteases of lysosomes and calpain family, which does not affect the expression level of Homer1a. A. Densities of Homer1c puncta along dendrites, expressed relative to the control. B. Total fluorescence intensities of immuno-labeled Homer1c in dendrites, expressed relative to the control. MG132 and E64d were added to the media from DMSO stock solutions, and the final concentration of DMSO was 0.1%. 'DMSO' represents treatments with 0.1% DMSO for 10 h. Error bars represent ± SEM ($n = 4–8$ dendrites). *$P < 0.01$ by Student's t-test.

examined the effects of BDNF (100 ng/ml for 4 h, Sigma) and MG132 (10 μM for 10 h, Peptide Institute Inc.) on the distribution of Homer1c. For comparison, we also used E64d (10 μM for 10 h, Peptide Institute), an inhibitor of proteases of lysosomes and calpain family, which has been shown not to affect the expression level of Homer1a [1]. As shown in Fig. 4, treatments with BDNF and MG132, but not E64d, resulted in significant reductions in the number of Homer1c puncta, without significantly affecting the total amounts of Homer1c, suggesting that endogenously accumulated Homer1a caused dispersion of Homer1c clusters.

The application of BDNF or MG132 showed apparently more distinct effects than the overexpression of Homer1a (Figs. 2 and 4). This may be due to the activation of MAP kinase by BDNF or MG132, but not by the Homer1c overexpression alone, that promotes the synaptic targeting of Homer1a to effectively disperse Homer1c [4].

The present results strongly suggest that not only exogenously expressed Homer1a but also endogenously induced Homer1a modulate the distribution of Homer1c and dendritic spine morphology. We have previously shown that membrane depolarization or stimulations of cells with phorbol esters or BDNF cause accumulation of Homer1a at postsynaptic regions [4,5]. Taken together, these observations suggest an important role of Homer1a in facilitation of synaptic remodeling. Strong synaptic activity causes upregulation and accumulation of Homer1a at postsynaptic sites, which in turn facilitate redistribution of Homer1c and reorganization of postsynaptic structures.

Acknowledgements

This work was supported by Grants-in-Aid for Scientific Research from the Ministry of Education, Science, Sports and Culture, Japan.

References

[1] H. Ageta, A. Kato, S. Hatakeyama, K. Nakayama, Y. Isojima, H. Sugiyama, Regulation of the level of Vesl-1S/Homer-1a proteins by ubiquitin-proteasome proteolytic systems, J. Biol. Chem. 276 (2001) 15893–15897.

[2] J. Beneken, J.C. Tu, B. Xiao, M. Nuriya, J.P. Yuan, P.F. Worley, D.J. Leahy, Structure of the Homer EVH1 domain-peptide complex reveals a new twist in polyproline recognition, Neuron 26 (2000) 143–154.

[3] P.R. Brakeman, A.A. Lanahan, R. O'Brien, K. Roche, C.A. Barnes, R.L. Huganir, P.F. Worley, Homer: a protein that selectively binds metabotropic glutamate receptors, Nature 386 (1997) 284–288.

[4] A. Kato, Y. Fukazawa, F. Ozawa, K. Inokuchi, H. Sugiyama, Activation of the ERK cascade promotes the accumulation of Vesl-1S/Homer-1a immunoreactivity at synapses, Mol. Brain Res. 118 (2003) 33–44.

[5] A. Kato, T. Fukuda, Y. Fukazawa, Y. Isojima, K. Fujitani, K. Inokuchi, H. Sugiyama, Phorbol esters promote postsynaptic accumulation of Vesl-1S/Homer-1a protein, Eur. J. Neurosci. 13 (2001) 1292–1302.

[6] A. Kato, F. Ozawa, Y. Saitoh, Y. Fukazawa, H. Sugiyama, K. Inokuchi, Novel members of the Vesl/Homer family of PDZ proteins that bind metabotropic glutamate receptors, J. Biol. Chem. 273 (1998) 23969–23975.

[7] A. Kato, F. Ozawa, Y. Saitoh, K. Hirai, K. Inokuchi, Vesl, a gene encoding VASP/Ena family related protein, is upregulated during seizure, long-term potentiation and synaptogenesis, FEBS Lett. 412 (1997) 183–189.

[8] C. Sala, K. Futai, K. Yamamoto, P.F. Worley, Y. Hayashi, M. Sheng, Inhibition of dendritic spine morphogenesis and synaptic transmission by activity-Inducible protein Homer1a, J. Neurosci. 23 (2003) 6327–6337.

[9] C. Sala, V. Piech, N.R. Wilson, M. Passafaro, G.S. Liu, M. Sheng, Regulation of dendritic spine morphology and synaptic function by Shank and Homer, Neuron 31 (2001) 115–130.

[10] M. Sato, K. Suzuki, S. Nakanishi, NMDA receptor stimulation and brain-derived neurotrophic factor upregulate Homer 1a mRNA via the mitogen-activated protein kinase cascade in cultured cerebellar granule cells, J. Neurosci. 21 (2001) 3797–3805.

[11] J. Sun, S. Tadokoro, T. Imanaka, S.D. Murakami, M. Nakamura, K. Kashiwada, J. Ko, W. Nishida, K. Sobue, Isolation of PSD-Zip45, a novel Homer/vesl family protein containing leucine zipper motifs, from rat brain, FEBS Lett. 437 (1998) 304–308.

[12] S. Usui, D. Konno, K. Hori, H. Maruoka, S. Okabe, T. Fujikado, Y. Tano, K. Sobue, Synaptic targeting of PSD-Zip45 (Homer 1c) and its involvement in the synaptic accumulation of F-actin, J. Biol. Chem. 278 (2003) 10619–10628.

[13] B. Xiao, J.C. Tu, R.S. Petralia, J.P. Yuan, A. Doan, C.D. Breder, A. Ruggiero, A.A. Lanahan, R.J. Wenthold, P.F. Worley, Homer regulates the association of group 1 metabotropic glutamate receptors with multivalent complexes of homer-related, synaptic proteins, Neuron 21 (1998) 707–716.

Appl Microbiol Biotechnol (2004) 64: 531–536
DOI 10.1007/s00253-003-1544-8

K. Sugiyama · T. P. Niki · K. Inokuchi · Y. Teranishi ·
M. Ueda · A Tanaka

Heterologous expression of metabotropic glutamate receptor subtype 1 in *Saccharomyces cerevisiae*

Received: 12 August 2003 / Revised: 28 November 2003 / Accepted: 5 December 2003 / Published online: 22 January 2004

Abstract The upstream region of the isocitrate lyase gene (UPR-ICL) from the *n*-alkane-utilizing yeast *Candida tropicalis* serves as a useful promoter of gene expression in the yeast *Saccharomyces cerevisiae*. The production of rat metabotropic glutamate receptor 1α (mGluR1α), which belongs to the G-protein-coupled receptor (GPCR) family, was tested under the control of UPR-ICL. Expression of mGluR1α was found in recombinant clones and enhanced by replacing the signal sequence of mGluR1α with the corresponding region of the α-factor receptor (Ste2), which is a GPCR found in *S. cerevisiae*. Moreover, the membrane fraction from a recombinant clone associated with Vesl-1S/Homer-1a protein binds the mGluR1α in rat cerebellum. These results suggest that the UPR-ICL-controlled gene expression system is useful for heterologous GPCRs in *S. cerevisiae*.

Introduction

The G-protein coupled receptor (GPCR) is divided into seven regions where it crosses the cell membrane and responds to external stimuli through specific ligand binding. Eukaryote cells use GPCRs to receive and transduce the signals in networks. GPCRs are perhaps the most widespread pharmacological targets, thus research into structural sites and molecules that interact with GPCRs is of particular importance.

The metabotropic glutamate receptor 1α (mGluR1α), whose activity is enriched in hippocampus and cerebellum (Martin et al. 1992), is member of the GPCR superfamily, and modulate postsynaptic calcium release from internal stores (Fangi et al. 2000). Recent work has shown that Vesl/Homer proteins bind the intracellular C terminus of mGluR1α and thus may regulate the function of the receptor (Kato et al. 1998; Minami et al. 2003). The Vesl-

K. Sugiyama · T. P. Niki · Y. Teranishi
GenCom,
11 Minamiooya,
Machida 194-8511, Japan

K. Inokuchi
Mitsubishi Kagaku Institute of Life Sciences,
11 Minamiooya,
Machida 194–8511, Japan

M. Ueda · A. Tanaka
Laboratory of Applied Biological Chemistry, Department of Synthetic Chemistry and Biological Chemistry, Graduate School of Engineering, Kyoto University,
Yoshida,
Sakyo-ku, Kyoto 606-8501, Japan

Present address:
K. Sugiyama (✉)
Division of Microbiology, National Institute of Health Sciences,
1-18-1 Kamiyoga,
Setagaya-ku, Tokyo 158-8501, Japan
e-mail: sugiyama@nihs.go.jp
Tel.: +81-3-37009496
Fax: +81-3-37009496

Present address:
T. P. Niki
Business Development Department, Amniotec,
2-21-7 Akasaka,
Minato-ku, Tokyo 107-0052, Japan

Present address:
Y. Teranishi
Medical Science and Business Liaison Office, Kyoto University,
Yoshida Sakyo-ku, Kyoto 606-8501, Japan

Present address:
M. Ueda
Laboratory of Biomacromolecular Chemistry, Department of Applied Biochemistry, Division of Applied Life Sciences, Graduate School of Agriculture Sakyo-ku, Kyoto University,
Kitashirakawa-Oiwake-cho,
Kyoto 606-8502, Japan

Present address:
A. Tanaka
Department of Applied Chemistry, College of Engineering, Chubu University,
Kasugai-shi, Aichi 487-8501, Japan

1S/Homer-1a protein, a member of the Vesl/Homer family, is up-regulated after induction of long-term potentiation (LTP) and binds the metabotropic glutamate receptor's C terminus in the intracellular domain (Kato et al. 1997, 1998). Thus, it is important to investigate proteins that bind mGluR1α in order to understand the mechanism of LTP.

In the present study, we describe an expression system for the heterologous production of rat mGluR1α. The yeast *Saccharomyces cerevisiae* is as an attractive host for producing large quantities of heterologous proteins because the cells can be grown to high cell concentrations in inexpensive media. Additionally, when an expression vector in which the upstream region of the isocitrate lyase gene (UPR-ICL) from the *n*-alkane-utilizing yeast *Candida tropicalis* serves as a promoter was introduced into *S. cerevisiae*, heterologous gene expression under control of the UPR-ICL was enhanced in the stationary phase and during growth on media containing a non-fermentable carbon source (Uemura et al. 1995). Here, we also report on the production of rat mGluR1α using a UPR-ICL-controlled gene expression system in *S. cerevisiae*.

Materials and methods

Strains and media

Escherichia coli DH5α (F⁻, *endA1*, *hsdR17*(r_k^-, m_k^-), sup E44, *thi-1*, λ⁻, *recA1*, *gyrA96*, Ø 80 d *lacZ*DM15) was used as host for recombinant DNA manipulation. *S. cerevisiae* MT8-1 (*MAT*a *ade his3 leu2 trp1 ura3*) (Tajima et al. 1985) was used as a host for protein production. Yeast was cultivated on YPD medium (1% yeast extract, 2% peptone, 2% glucose), SD minimum medium (2% glucose, 0.67% yeast nitrogen base without amino acids; pH 5.5) with appropriate amino acids.

Disruption of *STE2*

To delete *STE2* , an *EcoRI*/*Bam*HI DNA fragment was subcloned upstream of the *STE2* coding region amplified from *S. cerevisiae* genomic DNA by PCR using primers (5'-CTGCCAAAAT-GAATTCTCACACGCTGTAGT-3' and 5'-ATACTAATAGG-GATCCTTAAATAGTATTCC-3'), and an *Xho*I/*Bam*HI DNA fragment from the 3' end of the coding region amplified by PCR using primers (5'-CATCCTCGCCTCGAGTTTGGAACCAAAC-CAGGG-3' and 5'-TCTCTATATCATCTGAAT- TCTCAGAAA-CAA-3') into vector pRS403 (Sikorski and Hieter 1989). The resulting plasmid (p403Dste2) was cut with *Eco*RI and transformed into *S. cerevisiae* strain MT8-1 strain. Transformants with $HIS3^+$ phenotype were isolated, and disruption of chromosomal *STE2* was confirmed by PCR.

Construction of mGluR1α expression vectors

The construction of rat mGluR1α expression plasmid, pWMG1, was initiated by inserting a *Bgl*II/*Nco*I fragment encoding the 5' half of the mGluR1α ORF, amplified from pmGR1 containing mGluR1α cDNA (Masu et al. 1991), into vector pWI3 by PCR using primers 5'-GCCGGACCATAGATC-TATGGTCCGGCTCCTCTTGAT-3' and 5'-AGCCCATGTGC-CATGGCATAGATGGCATTGATGACA-3' (Kanai et al. 1996). A DNA fragment containing the 3' half of the mGluR1α ORF was prepared by PCR using primers (5'-GCCATCTATGCCATGGCA-CATGGGCTGCAGAACATG-3' and 5'-CACCCTGTAGCTC-GAGCTACAGGGTGGAAGAGCTTT-3') with pmGR1 as a template, followed by digestion with *Nco*I and *Xho*I. This fragment was inserted into pWI3 containing the 5' half of the mGluR1α ORF digested with *Nco*I and *Xho*I. The resulting plasmid was named pWMG1(Fig. 1A). To replace the mGluR1α signal sequence (Masu et al. 1991) with Ste2 (Gaibelet et al. 1999), a DNA fragment containing Ste2 signal sequence was prepared by PCR using primers (5'-GCATCAGACATAGATCTATGTCTGATGCGGCTCCTT-CATTGAGCAATCTATTTTATGATCCAACGTATAGGATGCCT-GACAGAAAAGTATTGCTGGCA-3' and 5'-AGCCCATGTGC-CATGGCATAGATGGCATTGATGACA-3') with pmGR1 as a template, followed by digestion with *Bgl*II and *Nco*I. The *Bgl*II/*Nco*I fragment of plasmid pWMG1 was substituted with this newly synthesized fragment to produce plasmid pWSMG1 (Fig. 1B).This resulted in the replacement of the 20 amino-terminal codons of mGluR1α cDNA by the 17 amino-terminal codons of *STE2*. These constructed plasmids were verified by DNA sequencing.

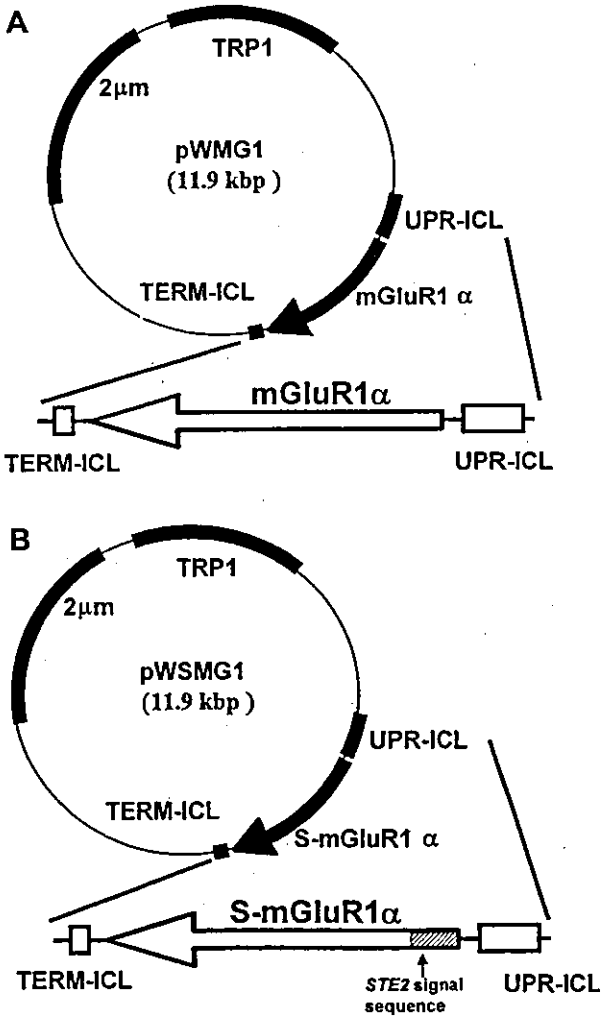

Fig. 1A, B Expression plasmids for mGluR1α and S-mGluR1α. A Expression map of plasmid pWMG1. The UPR-ICL promoter controls the expression of native mGluR1α. B Expression map of plasmid pWSMG1. The signal sequence of mGluR1α is replaced by the corresponding region of *STE2*

Construction of Vesl-1S-GFPuv4 fusion protein expression vector

For the construction of the expression vector pI4B, PCR was used to introduce a multiple cloning site (MCS), an enterokinase recognition site (ERS), and His_6 on a GFPuv4 coding region (Ito et al. 1999) from plasmid pGFPTA (Ito et al. 2000). Primer 5′-GGTACCA-GATCTGGTACCATCGATGGGCCCGGGGACGATGACGATAA-GATGAGTAAAGGAGAAGAACTTTTCACTGGAGTTGTCC-CAATTCTTGTT-3′, which contained a *Bgl*II site and was hybridized at the N-terminal of GFPuv4, was used to introduce *Kpn*I, *Cla*I, *Apa*I, and *Sma*I sites and ERS. 5′-TGAAGATCTT-CAATGGTGATGGTGATGATGTGATTTGTAGAGCTCATC-CATGCCATGTGTAATCCCAGCAGCAGTTACAAA-3′, which contains a *Bgl*II site and was hybridized at the C-terminal of GFPuv4, was used to introduced a His_6. The PCR fragment digested with *Bgl*II was inserted into the *Bgl*II site of pWI3 to give plasmid pI4B. The sequence of the amplified *Bgl*II/*Bgl*II fragment from pI4B was confirmed by DNA sequencing. To construct plasmid pGV1S for the expression of Vesl-1S-GFPuv4 fusion protein using pI4B, PCR was used to introduce an *Apa*I site at both ends of rat Vesl-1S cDNA (28 kDa) (Kato et al. 1997). The primer 5′-GTTCCCCCATGGGCCCATGGGGGAACAACCTATCTT-3′, containing an *Apa*I site, was hybridized at the N-terminal of rat Vesl-1S cDNA. Primer 5′-CATGATTAAAGGGCCCTTTAATCAT-GATTGCTGAAT-3′, containing an *Apa*I site, was hybridized at the C-terminal of Vesl-1S cDNA. The amplified fragment was cut with *Apa*I and inserted at the *Apa*I site of pI4B (Fig. 2A). The sequence of the amplified *Apa*I/*Apa*I fragment from pGV1S was confirmed by DNA sequencing.

Isolation of membranes

Yeast cells transformed with pWMG1 or pWSMG1 were inoculated in 20 ml YPD medium and cultured for the indicated time at 30°C with shaking (200 rpm). The cells were then collected by centrifugation and rinsed once with water. The pellet was suspended in TES buffer (10 mM Tris-HCl, pH 7.5; 1 mM EDTA; 10% sucrose) containing protease inhibitor cocktail for yeast (Sigma). The suspension was vortexed with glass beads (17 g; mesh 400–600; Sigma) at 4°C for 5 min and then centrifuged at 3,000 *g* for 10 min to remove cell debris. The supernatant was centrifuged at 35,000 *g* for 60 min. The resulting membrane pellet was suspended in 0.2 ml TES buffer and stored at −80°C for further experiments.

Preparation of cerebellum from rat

A Wister rat (10 weeks) was killed, and the cerebellum was dissected and homogenized with a Polytron homogenizer (Kinematica, Littau, Switzerland) in extraction buffer (50 mM Tris-HCl, pH 6.8; 8 M urea; 2% SDS) supplemented with protease inhibitor cocktail for tissue extracts (Sigma) at 4°C. The homogenates were stored at −80°C for further experiments.

Western blot analysis

The production of mGluR1α was analyzed in cells that were grown for the indicated times. The membrane was diluted to a protein concentration of 15 μg/μl in TES buffer and boiled for 5 min with 2× SDS-loading buffer (Nakarai tesq, Kyoto, Japan). The membrane proteins were separated on a 5% SDS polyacrylamide gel (Laemmli 1970). Subsequently, proteins were transferred onto a polyvinylidendifluoride membrane (Towbin et al. 1979) and probed with rabbit anti-mGluR1 antibody (Upstate Biotechnology, Lake Placid, N.Y., USA) diluted 1/1,000. The blot was incubated with anti-rabbit IgG linked to horseradish peroxidase diluted 1/5,000, and the immunoreactive proteins were detected by a Bio-Rad Chemi Doc system.

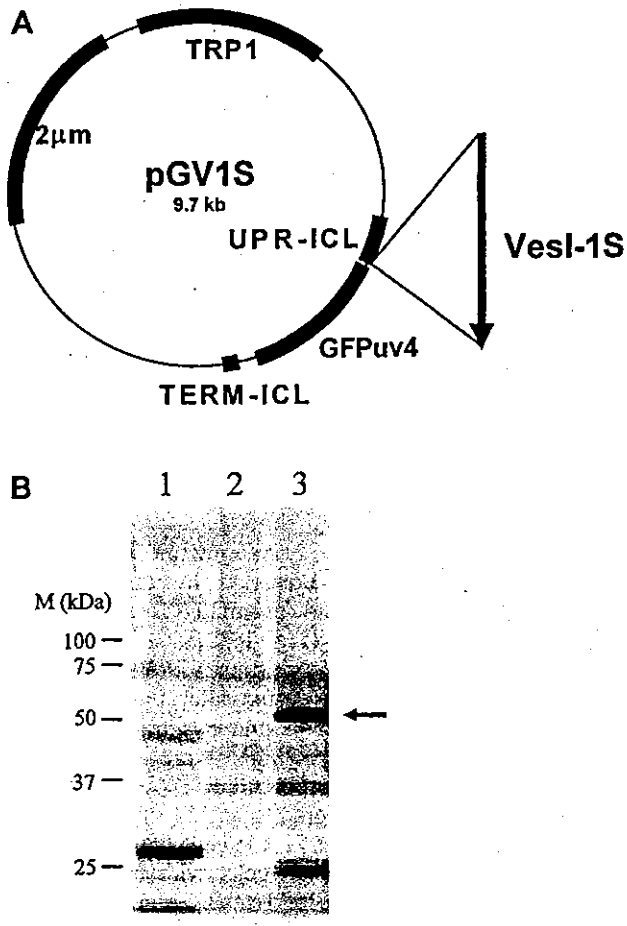

Fig. 2 Construction of plasmid pGV1S for the expression of Vesl-1S-GFPuv4 (A), and Western blot analysis of recombinant Vesl-1S-GFPuv4 produced by cells harboring pGV1S (B). An aliquot (3 μg) of each cell-free extract was applied to an SDS-polyacrylamide gel (B). Anti-Homer-1a antibody was used to detect Vesl-1S-GFPuv4. *Lane1* Rat cerebellum (10 μg), *lane 2* pI4B, *lane 3* pGV1S. *Arrow* Vesl-1S-GFPuv4

Preparation of Vesl-1S-GFPuv4

S. cerevisiae MT8-1 cells carrying pGV1S plasmid were grown in 50-ml portions of YPD medium for 68 h. The yeast cells were then centrifuged and rinsed once with water. The pellet was suspended in 50 mM Tris-HCl, pH 7.5, containing protease inhibitor cocktail for yeast (Sigma). The suspension was vortexed with glass beads at 4°C for 5 min and then centrifuged at 3,000 *g* for 10 min. To confirm Vesl-1S-GFPuv4 expression, the resulting supernatant were separated on a 10% SDS polyacrylamide gel and electrophoretically transferred to polyvinylidendifluoride membrane. Immobilized proteins were probed with anti-Homer-1a (Santa Cruz Biotechnology Santa Cruz, Calif., USA) at 1/100 dilution and visualized using horseradish peroxidase-conjugated anti-goat IgG (Santa Cruz Biotechnology) diluted 1/4,000.

Immunoprecipitation

A membrane fraction of yeast cells carrying pWSMG1 and Vesl-1S-GFPuv4 was mixed with Protein G Sepharose (Amersham Pharmacia Biotech)-bound anti-mGluR1 antibody. After incubation at 4°C for 1 h, the resin was washed three times with 20 mM Tris-HCl, pH 7.5, containing 150 mM NaCl and 1% Triton X-100. The bound proteins were eluted from the resin by boiling in 40 µl SDS-loading buffer. The eluate (20 µl) was separated electrophoretically on an 8% SDS-polyacrylamide gel and blotted with anti-Homer-1a (Santa Cruz Biotechnology) diluted 1/100. Horseradish peroxidase-conjugated anti-goat IgG (Santa Cruz Biotechnology) diluted 1/4,000 was used as the secondary antibody. The immunosignal was visualized with a Bio-Rad Chemi Doc system.

Results

Time courses of mGluR1α expression

To examine the expression of rat mGluR1α using the pWI3 expression vector controlled by the UPR-ICL promoter, the coding region of mGluR1α was placed under control of UPR-ICL (Fig. 1A). *S. cerevisiae* cells transformed with pWMG1 were grown in YPD medium. The membrane proteins harvested after induction were separated on 5% SDS-polyacrylamid gels, transferred onto Immobilon sheets, and the blots were probed with polyclonal antibody against mGluR1. As shown in Fig. 3A, a protein band migrating at 142 kDa appears at 96 h in wild-type cells and at 71 h in cells with *ste2ΔHIS3* (Fig. 4A). When *S. cerevisiae* cells with pWMG1were cultivated, recombinant mGluR1α was produced transiently. A time-course experiment showed that S-mGluR1α expressed by pWSMG1 was first detected at 71 h and reached a maximum level at 125 h followed by a gradual decline (Fig. 3B). pWSMG1 encodes a mGluR1α cDNA in which the amino-terminal part of the receptor is replaced with the corresponding region of *STE2*, encoding an α-factor receptor belonging to the GPCR family in *S. cerevisiae*. By contrast, *ste2ΔHIS3* cells harboring plasmid pWSMG1 expressed S-mGluR1α first at 71 h, after which the amount of S-mGluR1α increased (Fig. 4B). These results suggest that the signal sequence of Ste2 enhanced mGluR1α expression on yeast membrane, and the disruption of *STE2* did not result in improved production of mGluR1α in yeast.

S-mGluR1α expressed in yeast cells that have interacted with Vesl-1S-GFPuv4

It was reported that mGluR1α interacts with Vesl-1S (Kato et al. 1998). We employed immunoprecipitation between S-mGluR1α, which is expressed on yeast membrane better than native mGluR1α, and Vesl-1S to confirm the function of S-mGluR1α on yeast membrane. As shown in Fig. 2B, yeast cells harboring pGV1S, comprising rat Vesl-1S cDNA inserted into the MCS of pI4B, produced Vesl-1S-GFPuv4 fusion protein. Anti-Homer-1a antibodies were used for immunoblotting of immunoprecipitates from the

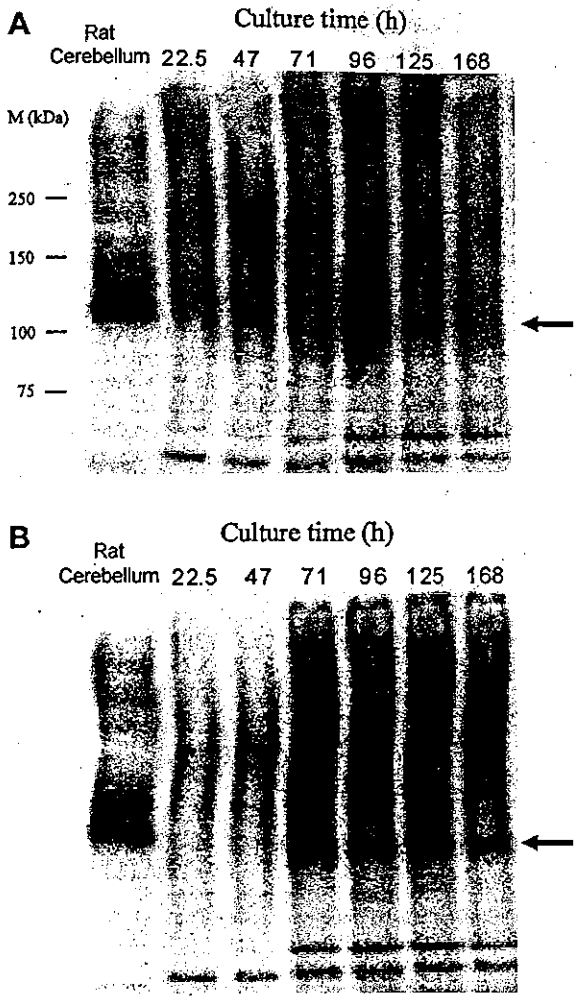

Fig. 3 Western blot analysis of membranes isolated from *Saccharomyces cerevisiae* wild-type cells transformed with pWMG1 (A) and pWSMG1 (B)

mixture of membrane fractions containing S-mGluR1α and cell lysates prepared from yeast cells transformed with pGV1S. The results showed that, using anti-mGluR1 antibodies, S-mGluR1α co-immunoprecipitated with Vesl-1S-GFPuv4 (Fig. 5), demonstrating that S-mGluR1α is associated with Vesl-1S.

Discussion

mGluR1α, which belongs to the GPCR family and is localized in the hippocampus, plays a role in synaptic plasticity. Recent studies reported that the C-termini of mGluR1α interact with Vesl-1S/Homer-1a, which has been isolated as synaptic plasticity-regulating protein. Elucidation of the molecular mechanism of synaptic plasticity requires a technique to functionally analyze the receptor.

In the present study, the expression of rat mGluR1α under the control of UPR-ICL was investigated. The results showed that mGluR1α expression using UPR-ICL

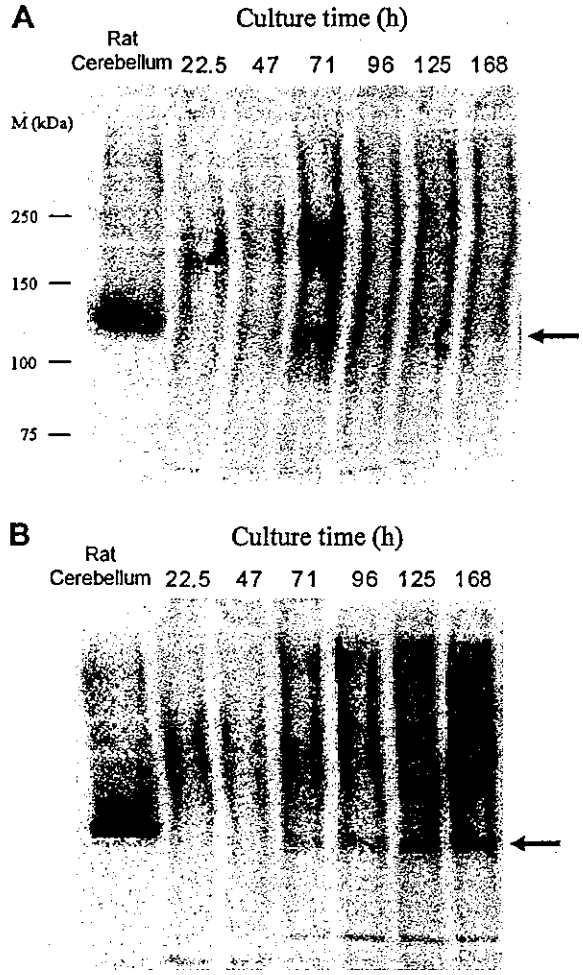

Fig. 4 Western blot analysis of membranes isolated from *S. cerevisiae ste2ΔHIS3* cells transformed with pWMG1 (A) and pWSMG1 (B)

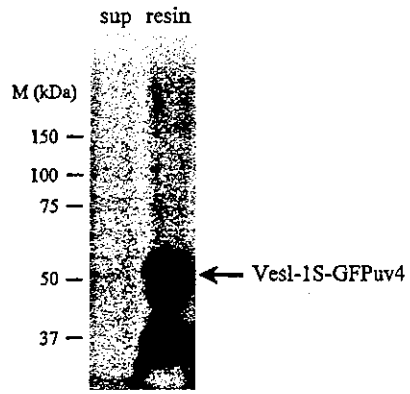

Fig. 5 Immunoprecipitation of S-mGluR1α and Vesl-1S-GFPuv4. Proteins retained from membranes of *S. cerevisiae ste2ΔHIS3* cells transformed with pWSMG1 were analyzed by Western blotting with anti-Homer-1a

is associated with the yeast membrane fraction, and higher expression levels were reached by replacing the signal sequence of the receptor with the corresponding region of *STE2*. Interaction between a signal sequence and a translocation channel of the endoplasmic reticulum (ER) leads to protein translocation into the ER (Jungnickel and Rapoport 1995). Replacing the signal sequence may facilitate translocation of S-mGluR1α to the ER thereby enhancing the efficiency of subsequent S-mGluR1α transport to the cytoplasmic membrane. Our result also show that S-mGluR1α produced by this system is associated in vitro with Vesl-1S-GPFuv4 expressed in yeast harboring pGV1S. Thus, the quantities produced by using this system are large enough to allow analysis at the biochemical level. The novel expression system using UPR-ICL and *STE2* signal sequence is attractive approach for producing heterologous GPCRs in yeast. Further studies will focus on its application as a component of a membrane-protein chip and for breeding yeasts that sense changes in their environmental condition. In addition, GFPuv4 fusion protein expressed by yeast carrying the pI4B vector should be applicable as indicators of protein-protein interactions, because the fluorescence of GFPuv4 is approximately 120-fold stronger than that of wild-type GFP (Ito et al. 1999).

Acknowledgements The authors are grateful to Shigetada Nakanishi (Kyoto University, Kyoto) for providing the mGluR1α cDNA, and to Yuzuru Husimi (Saitama University, Urawa) for providing the pGFPTA plasmid. We also thank Tomomi Sano for excellent technical assistance.

References

Fangi L, Chavis P, Ango F, Bockaert J (2000) Complex interactions between mGluRs, intracellular Ca_2^+ stores and ion channels in neurons. Trends Neurosci 23:80–88

Gaibelet G, Meilhoc E, Riond J, Saves I, Exner T, Liaubet L, Nürnberg B, Masson JM, Emorine LJ (1999) Nonselective coupling of the human μ-opioid receptor to multiple inhibitory G-protein isoforms. Eur J Biochem 261:517–523

Ito Y, Suzuki M, Husimi Y (1999) A novel mutant of green fluorescent protein with enhanced sensitivity for microanalysis at 488 nm excitation. Biochem Biophys Res Commun 264:556–560

Ito Y, Suzuki M, Husimi Y (2000) A T-extended vector using a green fluorescent protein as an indicator. Gene 245:59–63

Jungnickel B, Rapoport TA (1995) A posttargeting signal sequence recognition event in the endoplasmic reticulum membrane. Cell 82:261–270

Kanai T, Atomi H, Uemura K, Ueno H, Teranishi Y, Ueda M, Tanaka A (1996) A novel heterologous gene expression system in *Saccharomyces cerevisiae* using the isocitrate lyase gene promoter from *Candida tropicalis*. Appl Microbiol Biotechnol 44:759–765

Kato A, Ozawa F, Saitoh Y, Hirai K, Inokuchi K (1997) vesl, a gene encoding VASP/Ena family related protein, is upregulated during seizure, long-term potentiation and synaptogenesis. FEBS Lett 412:183–189

Kato A, Ozawa F, Saitoh Y, Fukazawa Y, Sugiyama H, Inokuchi K (1998) Novel members of the Vesl/Homer family of PDZ proteins that bind metabotropic glutamate receptors. J Biol Chem 273:23969–23975

Laemmli UK (1970) Cleavage of structural proteins during the assembly of the head of bacteriophage T4. Nature 227:680–685

Martin LJ, Blackstone CD, Huganir RL, Price DL (1992) Cellular localization of a metabotropic glutamate receptor in rat brain. Neuron 9:259–270

Masu M, Tanabe Y, Tsuchida K, Shigemoto R, Nakanishi S (1991) Sequence and expression of a metabotropic glutamate receptor. Nature 349:760–765

Minami I, Kengaku M, Smitt PS, Shigemoto R, Hirano T (2003) Long-term potentiation mGluR1 activity by depolarization-induced Homer1a in mouse cerebellar Purkinje neurons. Eur J Neurosci 17:1023–1032

Sikorski RS, Hieter P (1989) A system of shuttle vectors and yeast host strains designed for efficient manipulation of DNA in *Saccharomyces cerevisiae*. Genetics 122:19–27

Tajima M, Nogi Y, Fukasawa T (1985) Primary structure of the *Saccharomyces cerevisiae GAL7* gene. Yeast 1:67–77

Towbin H, Staehelin T, Gordon J (1979) Electrophoretic transfer of proteins from polyacrylamide gels to nitrocellulose sheets: procedure and some applications. Proc Natl Acad Sci USA 76:4350–4354

Uemura K, Atomi H, Kanai T, Teranishi Y, Ueda M, Tanaka A (1995) Effects of carbon source on the application of a novel foreign gene expression system in *Saccharomyces cerevisiae* using the upstream region of the *Candida tropicalis* isocitrate lyase gene (UPR-ICL). J Ferment Bioeng 80:529–533

THE JOURNAL OF BIOLOGICAL CHEMISTRY
Vol. 279, No. 36, Issue of September 3, pp. 37544–37550, 2004
Printed in U.S.A.

Stabilization of Exocytosis by Dynamic F-actin Coating of Zymogen Granules in Pancreatic Acini*[S]

Received for publication, April 9, 2004, and in revised form, June 2, 2004
Published, JBC Papers in Press, June 7, 2004, DOI 10.1074/jbc.M403976200

Tomomi Nemoto‡§¶, Tatsuya Kojima‡, Akihiro Oshima‡‖, Haruhiko Bito, and Haruo Kasai‡ ‡‡**

*From the ‡Department of Cell Physiology, National Institute for Physiological Sciences, and Graduate University of Advanced Studies (SOKENDAI), 5-1 Higashiyama, Myodaiji-cho, Okazaki, Aichi 444-8787, §Precursory Research for Embryonic Science and Technology (PRESTO), Japan Science and Technology Agency, 4-1-8 Honcho, Kawaguchi, Saitama 332-0012, the ‖Department of Otolaryngology, Kyoto Prefectural University of Medicine, Kamigyo-ku, Kyoto 602-0841, and the **Department of Neurochemistry, Faculty of Medicine, University of Tokyo, 7-3-1 Hongo, Tokyo 113-0033, and the ‡‡Center for Disease Biology and Integrative Medicine, Faculty of Medicine, University of Tokyo, 7-3-1 Hongo, Tokyo 113-0033, Japan*

Reorganization of F-actin in the apical region of mouse pancreatic acinar cells during Ca^{2+}-dependent exocytosis of zymogen granules was investigated by two-photon excitation microscopy with intact acini. Granules were rapidly coated with F-actin in response to either agonist stimulation or photolysis of a caged-Ca^{2+} compound. Such F-actin coating occurred exclusively at the surface of granules undergoing exocytosis and was prevented either by latrunculin-A, which inhibits actin polymerization, or by *Clostridium botulinum* exoenzyme C3, which inhibits the small GTPase Rho. Latrunculin-A or exoenzyme C3 also triggered the formation of vacuoles in acinar cells, a characteristic of acute pancreatitis. Stimulation of acini with high concentrations of cholecystokinin, which cause acute pancreatitis in mice, also impaired the F-actin coating of granules and induced vacuole formation. Latrunculin-A reduced the latency to exocytosis but did not affect the total number of exocytic events, suggesting that F-actin slows and further stabilizes exocytosis by facilitating F-actin coating. Rho-dependent F-actin coating of granule membranes thus stabilizes exocytic structures and is necessary for physiological progression of sequetial compound exocytosis in the exocrine pancreas and for prevention of acute pancreatitis.

Reorganization of the actin cytoskeleton plays an important role in a variety of cellular activities that range from cell migration and platelet aggregation to dendritic spine motility (1–3). Under resting conditions, the apical membrane of acinar cells in exocrine glands is coated with F-actin. Although this F-actin coat is thought to constitute a barrier to exocytosis (4–7), secretory granules undergo exocytosis selectively at the apical membrane (8–10). Redistribution of F-actin is induced during intense secretory activity (4, 11, 12), but it has remained unknown how F-actin regulates exocytosis in exocrine cells.

Reorganization of the actin cytoskeleton is also implicated in the pathogenesis of acute pancreatitis (13–16), which is characterized at the cellular level by the appearance of vacuoles in, and disruption of the polarized secretion of digestive enzymes from, pancreatic acinar cells (17). In animal models of this condition, protracted agonist stimulation results in both actin reorganization and vacuole formation (18–20). However, the relation between vacuole formation and F-actin reorganization has not been clarified.

Elucidation of the dynamic control of F-actin distribution during exocytosis in exocrine cells has not been possible by classical confocal microscopy because this technique lacks the tissue depth penetration necessary to visualize the fine organization of the apical plasma membrane within intact acini (10). In contrast, two-photon excitation microscopy has the ability to penetrate deep into tissues (10, 21) and allows simultaneous multicolor imaging with various combinations of fluorescent tracers (10, 49). Taking advantage of these attributes of two-photon excitation microscopy, we have now investigated actin dynamics associated with physiological and pathological exocytosis in pancreatic acinar cells.

EXPERIMENTAL PROCEDURES

Preparation of Mouse Pancreatic Acini—Clusters of acini were isolated from the pancreas of 5–7-week-old mice by a brief (4-min) digestion with collagenase (1 mg ml^{-1}; Wako, Osaka, Japan) followed by gentle trituration. The acini were dispersed in a small chamber and superfused (1 ml min^{-1}) with a solution (solution A) containing 150 mM NaCl, 5 mM KCl, 2 mM $CaCl_2$, 1 mM $MgCl_2$, 10 mM HEPES-NaOH (pH 7.3), and 10 mM glucose. For the experiment shown in Fig. 3, *G* and *H*, dispersed acini were cultured under an atmosphere of 5% CO_2 at 37 °C in Waymouth solution (Sigma) supplemented with penicillin (100 units ml^{-1}; Invitrogen), streptomycin (0.1 mg ml^{-1}; Invitrogen), 0.5 mM 3-isobutyl-1-methylxanthine (Sigma), soybean trypsin inhibitor (0.2 mg ml^{-1}; Sigma), and 2.5% fetal bovine serum (Invitrogen). The culture dishes were coated thickly with a collagen gel (MatriGel; BD Biosciences) to preserve cell polarity. All experiments done were approved by the Institutional Animal Care and Use Committee at Okazaki National Research Institutes.

Two-photon Excitation Imaging—For the visualization of exocytosis, pancreatic acini were immersed in solution A containing a fluid-phase polar tracer, either 0.5–1 mM sulforhodamine B (SRB[1]; Molecular Probes, Eugene, OR) or 0.5 mM cascade blue dextran (10 kDa; Molecular Probes). Cholecystokinin octapeptide (CCK; Peptide Institute, Osaka, Japan) was dissolved in solution A containing tracer and applied to cells through a glass pipette. All experiments were performed at room temperature (22–25 °C).

For the visualization of F-actin or G-actin, acini were fixed with 4%

* This work was supported by grants-in-Aid from the Ministry of Education, Culture, Sports, Science, and Technology of Japan, by Uehara Memorial Foundation, and by a research grant from the Human Frontiér Science Program Organization. The costs of publication of this article were defrayed in part by the payment of page charges. This article must therefore be hereby marked "*advertisement*" in accordance with 18 U.S.C. Section 1734 solely to indicate this fact.

[S] The on-line version of this article (available at http://www.jbc.org) contains three supplementary movies showing Two-photon imaging of sequential exocytosis of pancreatic acinus.

¶ To whom correspondence should be addressed. Tel.: 81-564-59-5873; Fax: 81-564-59-5874; E-mail: tn@nips.ac.jp.

[1] The abbreviations used are: SRB, sulforhodamine B; CCK, cholecystokinin; NP-EGTA, *o*-nitrophenyl EGTA; LatA, latrunculin-A.

paraformaldehyde in phosphate-buffered saline for 30 min, permeabilized with 0.1% Triton X-100 in phosphate-buffered saline for 10 min, washed with phosphate-buffered saline, and then stained with Alexa 488-phalloidin (0.17 μM; Molecular Probes) or Texas red-conjugated DNase I (0.3 μM; Molecular Probes) in phosphate-buffered saline. For the simultaneous imaging of both F-actin and fused granules, acini were immersed in a solution containing cascade blue dextran and stimulated for 1–10 min before fixation. latrunculin-A (LatA) (Molecular Probes) and cytochalasin D (Sigma) were first dissolved in dimethyl sulfoxide (10 mM; Sigma) and then diluted into solution A.

Two-photon excitation imaging of pancreatic acinar cells was performed as described (10). In brief, cells were imaged with an inverted microscope (IX70; Olympus, Tokyo, Japan) and a laser-scanning microscope (FV300, Olympus) equipped with a water-immersion objective lens (UPlanApo60× W/IR; numerical aperture, 1.2). A mode-locked Ti:sapphire laser (Tsunami, Spectra Physics) with an original pulse duration of 70–100 fs was attached to the laser port of the laser-scanning microscope; the group velocity dispersion of the microscope was compensated for by a set of chirp compensation optics. The laser power at the specimen was 4–5 milliwatts, and the excitation wavelength was 830 nm for SRB, fura-2FF, Alexa 488, and Texas red and 720 nm for cascade blue and Alexa 488.

The fluorescence of SRB or Texas red was measured at 570–650 nm, whereas that of fura-2FF or Alexa 488 was detected at 400–550 nm. For the double-staining experiments with Alexa 488 and cascade blue, the fluorescence was measured at 515–650 and 400–490 nm, respectively. Fluorescence was detected by photomultiplier tubes (R7683; Hamamatsu Photonics, Hamamatsu, Japan) in the FV300 microscope, and fluorescence images were acquired every 0.5–2 s. The fluorescence intensity of Alexa 488-phalloidin at the apical membrane was compared among preparations by quantifying fluorescence in the membrane region identified by cascade blue dextran imaging (see Fig. 2*A*). The 12-bit images were analyzed and color-coded with "fall," "gray," "green," or "red" look-up tables of the image acquisition and analysis software, either Fluoview of the FV300 microscope or IPLab Spectrum (Scanalytics, Fairfax, VA). Stacked images (see Figs. 1, *D–G*, 2, *A* and *E*, and 3) correspond to the maximum intensity plots reconstituted from a series of *xy* images along the *z* axis acquired by *xyz* scanning by the microscope in the "extended focus mode" of Fluoview software. Supplementary movie files were converted with QuickTime Pro software (Apple, Cupertino, CA).

For the simultaneous imaging of $[Ca^{2+}]_i$ and exocytosis, acini were preloaded for 30 min with fura-2FF-AM (20 μM; TEF Labs, Dallas, TX) in solution A. The $[Ca^{2+}]_i$ values were calculated from the fluorescence of fura-2FF as described (10). A mercury lamp (U-YLS100HG, Olympus) was used as an actinic light source for the caged-Ca^{2+} compound *o*-nitrophenyl EGTA (NP-EGTA). The lamp was connected to a two-port light guide (IX-RFA-caged, Olympus). The radiation from the actinic light was filtered by a UV band-pass filter (320–360 nm) and gated (250 ms) through an electric shutter (IX-ESU, Olympus). A rapid increase in $[Ca^{2+}]_i$ was triggered by UV photolysis of NP-EGTA, which was preloaded by incubation of acini with 10 μM NP-EGTA-AM (Molecular Probes) in solution A for 30 min.

RESULTS

Rapid F-actin Coating of Zymogen Granules—Two-photon excitation imaging allows direct visualization of zymogen granule exocytosis in pancreatic acini (Fig. 1, *A* and *C*) that have been immersed in a solution containing the polar tracer SRB, given that the tracer rapidly diffuses into individual granules that have fused with the plasma membrane (10). Two-photon imaging also allows simultaneous monitoring of the intracellular free Ca^{2+} concentration ($[Ca^{2+}]_i$) (Fig. 1*B*). CCK (100 pM) induced micromolar increases in $[Ca^{2+}]_i$, which in turn triggered pronounced exocytosis of zymogen granules at the apical membrane of acinar cells in a sequential manner. Granules present within deeper layers of the cell thus frequently underwent exocytosis by fusing with the Ω-shaped profiles of granules that had already fused with the apical membrane, resulting in the formation of grapelike clusters of fused structures (Fig. 1*C*; see Supplementary Movie 1) (10). The Ω-shaped profiles of fused granules were stable for an average of ~3 min (see Fig. 5*C*).

To elucidate the molecular basis of this stability of the

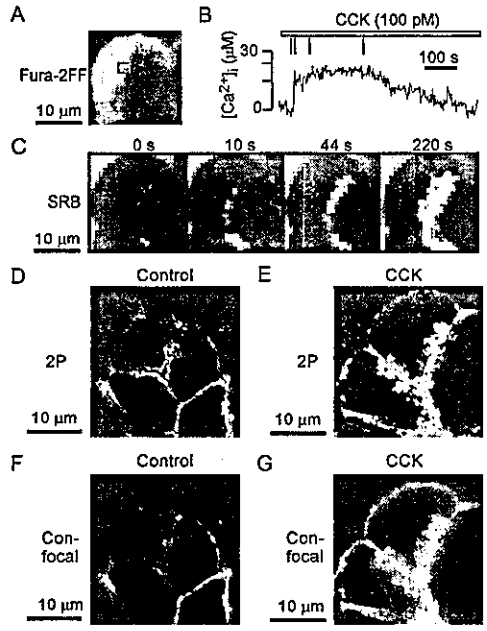

FIG. 1. **F-actin coating of zymogen granules.** *A*, a two-photon fluorescence image under resting conditions of a pancreatic acinus loaded with the acetoxymethyl ester (*AM*) of the Ca^{2+} indicator fura-2FF. *B*, the time course of $[Ca^{2+}]_i$ in the *boxed region* in *A* during stimulation with 100 pM CCK. *C*, two-photon imaging of SRB fluorescence of the acinus shown in *A*, which was exposed to a solution containing 0.5 mM SRB and stimulated with CCK. Images were acquired at the indicated times corresponding to the *vertical lines* in *B*. (See Supplementary Movie 1 for a real-time movie corresponding to these images.) *D* and *E*, two-photon (*2P*) imaging of Alexa 488-phalloidin staining of F-actin in nonstimulated cells (*D*) and in cells stimulated with 100 pM CCK for 60 s (*E*). These images represent stacks of *xy* images obtained at 10 consecutive *z* positions with an interval of 1 μm and located between 20 and 30 μm from the surface of the coverslip. *F* and *G*, one-photon confocal images of F-actin in the same acini shown in *D* and *E*, respectively. The images were obtained with the microscope and objective lens used in *D* and *E*, but fluorescence was excited with a CW laser at 488 nm instead of with a mode-locked laser at 830 nm.

Ω-shaped profiles, we investigated F-actin organization by staining of fixed preparations with Alexa 488-labeled phalloidin, which binds specifically to F-actin. In resting cells, a dense coat of F-actin was apparent at the apical membrane but not surrounding secretory granules (Fig. 1*D*) (22). After stimulation with 100 pM CCK, however, F-actin also coated secretory granules adjacent to the apical membrane (Fig. 1*E*). In contrast to the two-photon imaging, one-photon confocal microscopy was not able to detect such F-actin coating of granules (Fig. 1, *F* and *G*) as a result of the intense light scattering by zymogen granules (10), instead only revealing a rather diffuse spread of F-actin into the cytosol in response to CCK, as described in previous studies (11, 23).

To determine whether F-actin coating occurred selectively on granules undergoing exocytosis, we labeled exocytic profiles with a fixable fluorescent dextran (cascade blue dextran) during stimulation of acini with 100 pM CCK for 60 s and, after fixation, counterstained the cells with Alexa 488-phalloidin (Fig. 2*A*). The cluster of Ω-shaped profiles stained with cascade blue dextran (*red*) coincided exclusively with that of ring-like profiles of F-actin coats stained with Alexa 488-phalloidin (*green*). On average, 33% (4–50%, S.E. = 7%, n = 7 cells) of secretory granule areas at the apical pole of acinar cells, which were identified by negative staining with fura-2FF (10), was filled with exocytic granules, which were labeled with SRB during CCK stimulation for 10 min. These observations suggested that F-actin coating occurred selectively on all granules

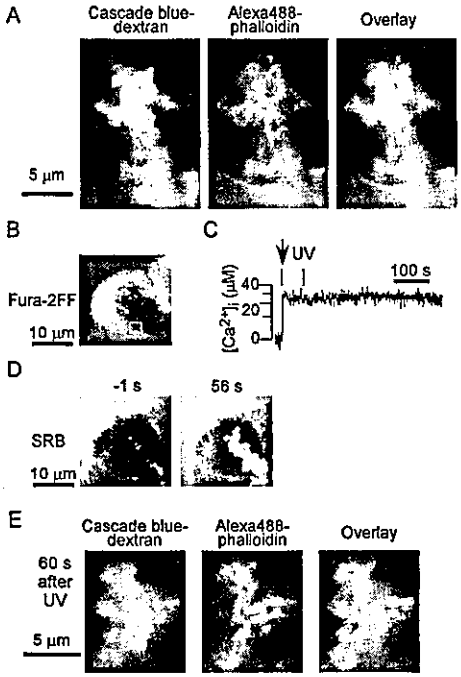

FIG. 2. **Selective F-actin coating of granules undergoing exocytosis.** *A*, double staining of granules with cascade blue dextran (*left*, *red*) and Alexa 488-phalloidin (*middle*, *green*) in acini stimulated with 100 pM CCK for 60 s; the overlaid image is shown on the *right*. These images were generated from stacks of *xy* images at 10 consecutive *z* positions with an interval of 1 μm. *B*, a fluorescence image under resting conditions of a pancreatic acinus loaded with fura-2FF-AM and NP-EGTA-AM. *Bar*, 10 μm. *C*, the time course of changes in $[Ca^{2+}]_i$ in the *boxed region* in *B* induced by UV photolysis. *D*, SRB fluorescence images of the acinus shown in *B*. Images were acquired at the indicated times corresponding to the *vertical lines* in *C*. *E*, double staining of granules with cascade blue dextran (*red*) and Alexa 488-phalloidin (*green*) in an acinus 60 s after UV-induced photolysis of NP-EGTA. The images were generated from a stack of 10 images, with each section being separated by 1 μm.

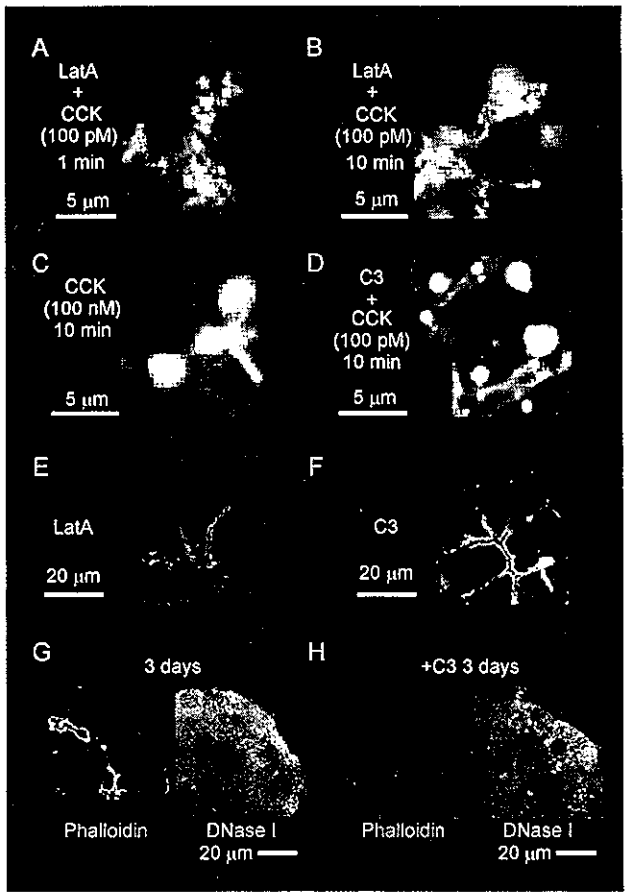

FIG. 3. **Mechanism of F-actin coating of granule and apical plasma membranes.** *A–D*, acini that had been pretreated with 10 μM LatA for 30 min before stimulation for 1 min (*A*) or 10 min (*B*) with 100 pM CCK; stimulated with 100 nM CCK for 10 min (*C*); or pretreated with exoenzyme C3 (50 μg ml^{-1}) for 2 h before stimulation for 10 min with 100 pM CCK (*D*). *E* and *F*, Alexa 488-phalloidin fluorescence images of pancreatic acini at rest after treatment with LatA (10 μM, 30 min) (*E*) or with exoenzyme C3 (50 μg ml^{-1}, 2 h) (*F*). The images in *A–F* were generated from stacks of *xy* images at seven consecutive *z* positions with an interval of 1 μm. *Bars*, 20 μm. *G* and *H*, double staining of cultured acini with Alexa 488-phalloidin (*left*) and Texas red-conjugated DNase I (*right*) after incubation for 3 days in the absence (*G*) or presence (*H*) of exoenzyme C3 (50 μg ml^{-1}). The images shown were generated from a stack of 6–11 images, with each section being separated by 1 μm.

that underwent exocytosis. In these experiments, when exocytosis was followed in live cell, it was still active with a rate of 0.05–0.27 events/second/cell at the time of fixation (60 s). The observation that all of the granules undergoing exocytosis were coated with F-actin therefore suggests that the coating was induced within 3.7 s (1/0.27 s) after the onset of exocytosis.

Homogeneous and large increases in $[Ca^{2+}]_i$ (Fig. 2, *B* and *C*) induced by UV flash photolysis of a caged-Ca^{2+} compound, NP-EGTA, gave rise to sequential exocytosis (Fig. 2*D*) similar to that elicited by agonist stimulation (Fig. 1*C*), consistent with the notion suggested previously (10) that sequential exocytosis does not depend on gradients of $[Ca^{2+}]_i$. The granules undergoing exocytosis in response to photolysis of the caged-Ca^{2+} compound were also selectively coated with F-actin (Fig. 2*E*), indicating that neither receptor activation (24) nor spatial heterogeneity of $[Ca^{2+}]_i$ (25) is required for this phenomenon.

Mechanism of F-actin Coating—To examine the role of actin polymerization in the F-actin coating of granule membranes, we investigated the effects of LatA, a membrane-permeable inhibitor of actin polymerization that binds with high affinity to actin monomer (G-actin) (26). Pretreatment with LatA (10 μM, 30 min) prevented the F-actin coating of all granules that underwent exocytosis during stimulation of acini with 100 pM CCK for 1 min (Fig. 3*A*). Furthermore, large vacuoles were apparent in such preparations fixed 10 min after the onset of stimulation with CCK (Fig. 3*B*); these vacuoles were not coated with F-actin. The formation of similar vacuoles was seldom detected in acini not treated with LatA before stimulation with 100 pM CCK. It was, however, induced by high concentrations (10–100 nM) of CCK in the absence of LatA (Fig. 3*C*) (19), indicating that the F-actin coating of granules was impaired at such high doses of agonist, which are known to induce acute pancreatitis in mice (20).

The coating of granules with F-actin during stimulation with 100 pM CCK was found to require the small GTPase Rho, based on the observation that such coating was prevented by pretreatment of freshly isolated acini with *Clostridium botulinum* exoenzyme C3 (50 μg ml^{-1}) for 2 h (Fig. 3*D*). This bacterial enzyme inhibits the activity of Rho without affecting that of other members of the Rho subfamily of small GTPases such as Cdc42 or Rac (27). Stimulation of exoenzyme C3-pretreated acini with CCK also induced the formation of vacuoles, which were not coated with F-actin (Fig. 3*D*). The rapid Rho-dependent F-actin coating of granules undergoing exocytosis thus appeared to be necessary to prevent vacuole formation.

We found that actin polymerization occurred constitutively at the apical plasma membrane. The fluorescence intensity of Alexa 488-phalloidin-labeled F-actin at the apical membrane